Spectral Function Calculation for Strongly Correlating Systems

Dissertation

zur Erlangung des Doktorgrades

des Fachbereichs Physik

der Universität Hamburg

vorgelegt von
German Ulm
aus
Krasnoyarsk

Hamburg
2010

Gutachter der Dissertation	Prof. Dr. A. Lichtenstein
	Prof. Dr. M. Potthoff
Gutachter der Disputation	Prof. Dr. A. Lichtenstein
	Prof. Dr. E. Koch
Datum der Disputation	09 Juli 2010
Vorsitzender des Prüfungsausschusses	Dr. A. Chudnovskiy
Vorsitzender des Promotionsausschusses	Prof. Dr. Jochen Bartels
Dekan des Fachbereichs Physik	Prof. Dr. Heinrich Graener

Abstract

This thesis presents an efficient approach to calculate dynamical properties of solids with strong electron correlations. The fast cluster method, a so-called finite temperature Lanczos method is combined with the Dynamical mean-field theory (DMFT) in order to study orbital degenerate systems as function of temperature. The full local Coulomb interaction was taken into account in all calculations. A first application is two test systems: $5+1$ and $5+5$ Anderson impurity models.

In the case of $5+1$ Anderson impurity model it is possible to take into account a large number of eigenstates: $N_{arnoldi} > 100$. The chemical potential of the system μ were changed in a broad range which leads to a change of a multiplet structure of the spectrum. In all this range of chemical potential μ the ground state of the system is degenerate. At zero temperature it were found that the temperature Lanczos calculations reproduce the correct density of states obtained with exact diagonalization if one chooses the set of ground states which remains the symmetry of the system. If all degenerate ground states are taken into account than the temperature Lanczos method reproduces the correct density of states of the test systems with a good accuracy.

In the case of finite temperaure calculations electron transitions to higher energy levels become important. Therefore calculations with $N_{arnoldi} = 1$ do not reproduce the DOS obtained with exact diagonalitation at any parameters. One needs to consider not only the ground state but also low-energy excited states.

In the second part of the thesis the problem known as double-counting one for systems with strong electron correlations is considered. We conducted an extensive study of the charge transfer system NiO in the LDA+DMFT framework using quantum Monte Carlo and temperature Lanczos impurity solvers. By treating the double-counting correction as an adjustable parameter we systematically investigated the effects of different choices for the double counting on the spectral function. Different methods for fixing the double counting correction can drive the result from Mott insulating to al-

most metallic. We propose a reasonable scheme for determination of the double-counting corrections for insulating systems.

The last part of the thesis describes the application of the LDA+DMFT approach with the temperature Lanczos as impurity solver to the ferromagnetic nickel. The multiplet structure of full d-shell is taken into account. A satellite peak in spectral function is found around $-5\,eV$.

Zusammenfassung

In dieser Doktorarbeit soll eine effiziente Methode zur Berechnung dynamischer Eigenschaften von Festkrpern mit starken elektronischen Korrelationen prsentiert werden. Die Fast-Cluster-Methode, ein sogenanntes finite-temperature Lanczos, wurde mit der Dynamischen Molekularfeldtheorie (DMFT) kombiniert, um das Verhalten von Systemen mit entarteten Orbitalen in Abhngigkeit von der Temperatur zu untersuchen. In allen Rechnungen wurde die volle lokale Coulombwechselwirkung bercksichtigt. Als erste Anwendung wurden zwei Testsysteme untersucht:$5 + 1$ und $5 + 5$ Anderson-Impurity-Modelle.

Im Fall des $5 + 1$ Anderson-Impurity-Modells ist es mglich, eine groe Anzahl von Eigenzustnden zu bercksichtigen: $N_{arnoldi} > 100$. Das chemische Potential des Systems μ wurde ber einen groen Wertebereich hinweg variiert, was zu einer nderung der Multiplettstruktur des Spektrums fhrt. Im gesamten Wertebereich von μ ist der Grundzustand des Systems entartet. Es wurde festgestellt, da finite-temperature Lanczos die aus exakter Diagonalisierung erhaltene korrekte Zustandsdichte reproduziert wenn man einen Satz von Grundzustnden whlt die die Symmetrie des Systems wahren. Werden alle entarteten Grundzustnde des Systems mitbercksichtigt, so reproduziert finite-temperature Lanczos mit einer guten Genauigkeit die korrekte Zustandsdichte.

Im Falle endlicher Temperaturen gewinnen die bergnge von Elektronen zu hheren Energieniveaus an Bedeutung. Daher reproduzieren Rechnungen mit $N_{arnoldi} = 1$ fr keinen Satz von Parametern die korrekte Zustandsdichte. Es mssen zustzlich zu dem Grundzustand niederenergetische angeregte Zustnde mitbercksichtigt werden.

Im zweiten Teil dieser Arbeit wurde ein als Double-Counting bekanntes Problem fr Systeme mit starken elektronischen Korrelationen nher betrachtet. Wir fhrten im Rahmen von LDA+DMFT eine sorgfltige Untersuchung des charge-transfer-Systems NiO durch, und zwar unter Verwendung des Quantum Monte Carlo sowie des finite-temperature Lanczos Impurity Solvers. Indem wir die Double-Counting-Korrektur als einen einstellbaren

Parameter behandelten untersuchten wir deren Einfluss auf die Spektralfunktion. Unterschiedliche Methoden zur Bestimmung des Double-Countings knnen das Ergebnis von einem Mott-isolierenden bis hin zu einem nahezu metallischen Zustand ndern. Wir schlagen eine geeignete Methode zur Bestimmung des Double-Countings in einem isolierenden System vor.

Der letzte Teil dieser Arbeit beschreibt die Anwendung von LDA+DMFT mit dem finite-temperature Lanczos als Impurity Solver auf ferromagnetisches Nickel. Die Multiplett-Struktur der vollen d-Schale wird dabei mitbercksichtigt. Wir finden einen Satellit-Peak in der Spektralfunktion bei etwa $-5\,eV$.

Contents

Chapter 1

Introduction

Describing material properties from the "first principles" using only information about the atomic structure is a great challenge in theoretical physics. The starting point of the "theory of everything" is the Hamiltonian for the system of electrons and nuclei,

$$\hat{H} = \hat{H}_e + \hat{H}_i + \hat{H}_{ei} \tag{1.1}$$

where $\hat{H}_e$ describes the dynamics of electrons, $\hat{H}_i$ the ion core or nuclei, and $\hat{H}_{ei}$ their mutual interactions, . The Hamiltonian called "*ab-initio*" contains only the fundamental constants such as electronic charge, electronic and nuclei masses etc. The nonreletevistic version of this Hamiltonian reads:

$$\begin{aligned}\hat{H} = &-\frac{\hbar^2}{2m_e}\sum_i \nabla_i^2 - \sum_{i,I}\frac{Z_I e^2}{|\mathbf{r_i}-\mathbf{R_I}|} + \frac{1}{2}\sum_{i\neq j}\frac{e^2}{|\mathbf{r_i}-\mathbf{r_j}|} \\ &-\sum_I \frac{\hbar^2}{2M_I}\nabla_I^2 + \frac{1}{2}\sum_{I\neq J}\frac{Z_I Z_J e^2}{|\mathbf{R_I}-\mathbf{R_J}|},\end{aligned} \tag{1.2}$$

where e, m_e, $\boldsymbol{r}_i$ denote correspondingly electron charge, mass, coordinate and in analogy Z_I, M_I, $\boldsymbol{R}_I$ are ion charge, mass and coordinate.

It is essential to include the effects of difficult many-body terms, namely electron-electron Coulomb interactions and the complex structures of the nuclei that emerge from the combined effects of all the interactions. The goal of the theory of electronic structure calculations the development of methods to treat electronic correlations with sufficient accuracy that one can predict the diverse physical phenomena exhibited in matter, starting from (1.2). It is most informative and productive to start with the fundamental many-body theory.

There is only one type of term in the general Hamiltonian that can be regarded as "small", the ratio of electron mass to nuclei one m_e/M_I. A perturbation series can be defined in terms of this parameter which is expected

to have general validity for the full interacting system of electrons and nuclei. In the first order approximation in m_e/M_I the kinetic energy of the nuclei can be ignored. This is the Born-Oppenheimer or adiabatic approximation, which is an excellent approximation for many proposes, e.g. the calculation of nuclear vibrations modes in different solids. In other cases, it forms the starting point for perturbation theory in electron-phonon interactions which is the basis for understanding electrical transport in metals, polaron formation in insulators, certain metal-insulator transitions, and the BCS theory of superconductivity. In this work we focus on the Hamiltonian for the electrons, in which the positions of the nuclei are fixed.

Ignoring the nuclei kinetic energy, the fundamental Hamiltonian for the theory electronic structure can be written as

$$\hat{H} = \hat{T} + \hat{V}_{ext} + \hat{V}_{int} + E_{II} \tag{1.3}$$

If we adopt the Hartree atomic units $\hbar = m_e = 1$, then the different terms in (1.3) may be written the simplest form. The kinetic energy operator for the electrons $\hat{T}$ is

$$\hat{T} = -\frac{1}{2}\sum_i \nabla_i^2, \tag{1.4}$$

$\hat{V}_{ext}$ is the potential acting on the electrons due to the nuclei,

$$\hat{V}_{ext} = \sum_{i,I} V_I(|\mathbf{r_i} - \mathbf{R_I}|), \tag{1.5}$$

$\hat{V}_{int}$ is the electron-electron interaction,

$$\hat{V}_{int} = \frac{1}{2}\sum_{i\neq j} \frac{1}{|\mathbf{r_i} - \mathbf{r_j}|}, \tag{1.6}$$

and the final term E_{II} is the classical interaction of nuclei with one another and contribute to the total energy of the system but are not important for the problem of describing the electrons. Here the effect of nuclei the electrons is included in fixed potential "external" to the electrons. Other "external potentials", such as electric fields and Zeeman terms, can readily be included. Thus, for electrons, the Hamiltonian, (1.3), is central to the theory of electronic structure.

The fundamental equation governing a non-relativistic quantum system is the time-independent Schrödinger equation,

$$\hat{H}\Psi(\{\boldsymbol{r}_i\}) = E\Psi(\{\boldsymbol{r}_i\}), \tag{1.7}$$

where the many-body wave function for the electrons is $\Psi(\{r_i\}) \equiv \Psi(r_1, r_2, \ldots, r_N)$, the spin is assumed to be included in the coordinate r_i, and, of course, the wave function must be antisymmetric in the coordinates of the electrons $r_1, r_2, \ldots, r_N$.

The expression for any observable is an expectation value of an operator $\hat{O}$, which involves an integral over all coordinates,

$$\langle \hat{O} \rangle = \frac{\langle \Psi | \hat{O} | \Psi \rangle}{\langle \Psi | \Psi \rangle}. \tag{1.8}$$

The density of particles $n(\boldsymbol{r})$, which plays a central role in electronic structure theory, is given by the expectation value of the density operator $\hat{n}(\boldsymbol{r}) = \sum_{i=1,N} \delta(\boldsymbol{r} - \boldsymbol{r}_i)$,

$$n(\mathbf{r}) = \frac{\langle \Psi | \hat{n}(\mathbf{r}) | \Psi \rangle}{\langle \Psi | \Psi \rangle} = N \frac{\int d^3\mathbf{r}_2 \cdots d^3\mathbf{r}_N \sum_{\sigma_1} |\Psi(\mathbf{r}_1, \mathbf{r}_2, \ldots, \mathbf{r}_N)|^2}{\int d^3\mathbf{r}_2 \cdots d^3\mathbf{r}_N |\Psi(\mathbf{r}_1, \mathbf{r}_2, \ldots, \mathbf{r}_N)|^2}, \tag{1.9}$$

which has this form because of the symmetry of the wave function in all the electrons coordinates. (The density for each spin results if the sum over σ_1 is omitted.) The total energy is the expectation value of the Hamiltonian,

$$E = \frac{\langle \Psi | \hat{H} | \Psi \rangle}{\langle \Psi | \Psi \rangle} \equiv \langle \hat{H} \rangle = \langle \hat{T} \rangle + \langle \hat{V}_{int} \rangle + \int d^3\mathbf{r} V_{ext}(\mathbf{r}) n(\mathbf{r}) + E_{II}, \tag{1.10}$$

where the expectation value of the external potential has been explicitly written as a simple integral over the density function. The final term E_{II} is the electrostatic nucleus-nucleus (or ion-ion) interaction, which is essential only in the total energy calculation, but is just a classical additive term in the theory of electronic structure.

The eigenstates of the many-body Hamiltonian are stationary points (saddle points or the minimum) of the energy expression (1.10). These may be found by varying the ration in (1.10) or by the varying the nominator subject to the constraint of orthonormality ($\langle \Psi | \Psi \rangle = 1$), which can be done using the method of Lagrange multiplies,

$$\delta[\langle \Psi | \hat{H} | \Psi \rangle - E(\langle \Psi | \Psi \rangle - 1)] = 0. \tag{1.11}$$

This is equivalent to the well-known Rayleigh-Ritz principle that functional

$$\Omega_{RR} = \langle \Psi | \hat{H} - E | \Psi \rangle \tag{1.12}$$

is stationary at any eigensolution $|\Psi_m\rangle$. Variation of the bra $\langle \Psi |$ leads to

$$\langle \delta\Psi | \hat{H} - E | \Psi \rangle. \tag{1.13}$$

The ground state wave function Ψ_0 is the state with lowest energy, which can be determined , in principle, by minimizing the total energy with respect to all the parameters in $\Psi(\{\mathbf{r}_i\})$, with the constraint that Ψ must obey the particle symmetry and any conservation laws. Excited states are saddle points of the energy with respect to variations in Ψ.

Chapter 2

Density Functional Theory, Linear Muffin-Tin Orbitals

2.1 Thomas-Fermi approximation

The density functional theory of quantum systems is originated from the work of Thomas [1] and Fermi [2] written in 1927. Although their approximation is not accurate enough for present day electronic structure calculations, the approach illustrates the main idea of functional theory. In the original Thomas-Fermi method the kinetic energy of the system of electrons is approximated as an explicit functional of the density, idealized as noninteracting electrons in homogeneous gas with density equal to the local density at any given point. Both Thomas and Fermi neglected exchange and correlation among the electrons; however, this was extended by Dirac [3] in 1930, who formulated the local approximation for exchange still in use today. This leads to to the energy functional for electrons in an external potential $V_{ext}(r)$

$$\begin{aligned} E_{TF} =& C_1 \int d^3\mathbf{r}\, n(\mathbf{r})^{(5/3)} + \int d^3\mathbf{r}\, V_{ext}(\mathbf{r}) n(\mathbf{r}) \\ &+ C_2 \int d^3\mathbf{r},\ n(\mathbf{r})^{(4/3)} + \frac{1}{2}\int d^3\mathbf{r} d^3\mathbf{r}' \frac{n(\mathbf{r})n(\mathbf{r}')}{|\mathbf{r}-\mathbf{r}'|}, \end{aligned} \tag{2.1}$$

where the first term is the local approximation to the kinetic energy with $C_1 = \frac{3}{10}(3\pi^2)^{(2/3)} = 2.871$ in atomic units, the third term is the local exchange with $C_2 = -\frac{3}{4}(\frac{3}{\pi})^{(1/3)}$ and the last term is the classical electrostatic Hartree energy.

The ground state energy and electronic density can be found by minimizing the functional $E[n]$ in (2.1) for all possible $n(r)$ subject to the constraint

on the total number of electrons

$$\int d^3\mathbf{r}\, n(\mathbf{r}) = N. \tag{2.2}$$

Using the method of Lagrange multipliers, the solution can be found by an unconstrained minimization of the functional

$$\Omega_{TF}[n] = E_{TF}[n] - \mu \int d^3\mathbf{r}\, \{n(\mathbf{r}) - N\}, \tag{2.3}$$

where the Lagrange multiplier μ is the Fermi energy. For small variations of the density $\delta n(\mathbf{r})$, the condition for a stationary points is

$$\begin{aligned} &\int d^3\mathbf{r}\{\Omega_{TF}[n(\mathbf{r}) + \delta n(\mathbf{r})] - \Omega_{TF}[n(\mathbf{r})]\} \rightarrow \\ &\int d^3\mathbf{r}\{\frac{5}{3}C_1 n(\mathbf{r})^{2/3} + V(\mathbf{r}) - \mu\}\delta n(\mathbf{r}) = 0, \end{aligned} \tag{2.4}$$

where $V(\mathbf{r}) = V_{ext}(\mathbf{r}) + V_{Hartree}(\mathbf{r}) + V_x(\mathbf{r})$ is the total potential. Since (2.4) must be satisfied for any function $\delta n(\mathbf{r})$, it follows that the functional is stationary if and only if the density and potential satisfy the relation

$$\frac{1}{2}(3\pi^2)^{(2/3)} n(\mathbf{r})^{2/3} + V(\mathbf{r}) - \mu = 0. \tag{2.5}$$

2.2 The Hohenberg-Kohn theorems

The achievement of Hohenberg and Kohn is the formulation of density functional theory as an exact theory of many-body systems. The formulation applies to any system of interacting particles in external potential $V_{ext}(r)$, including any problem of electrons and fixed nuclei, where the Hamiltonian ca be written

$$\hat{H} = -\frac{\hbar^2}{2m_e}\sum_i \nabla_i^2 + \sum_i V_{ext}(\mathbf{r}_i) + \frac{1}{2}\sum_{i\neq j}\frac{e^2}{|\mathbf{r_i} - \mathbf{r_j}|}. \tag{2.6}$$

Density functional theory is based upon two theorems first provided by Hohenberg and Kohn [4].
Theorem 1: For any system of interacting particles in an external potential $V_{ext}(\mathbf{r})$, the potential $V_{ext}(\mathbf{r})$ is determined uniquely, except for a constant, by the ground state particle density $n_0(\mathbf{r})$.
Theorem 2: A universal functional for the energy $E[n]$ in terms of the density $n(\mathbf{r})$ can be defined, valid for any external potential $V_{ext}(\mathbf{r})$. For any

particular $V_{ext}(\mathbf{r})$, the exact ground state energy of the system is the global minimum value of this functional, and the density $n(\mathbf{r})$ that minimize the functional is the exact ground state density $n_0(\mathbf{r})$.

Density functional theory is the most widely used method today for electronic structure calculations because of the effective approach proposed by Kohn and Sham in 1965: to replace the original many-body problem by an auxiliary independent-particle problem. This ansatz, in principle, leads to exact calculations of many-body systems using independent-particle methods; in practice, it has made possible to approximate the DFT formulation that have proved to be remarkably successful. As a self-consistent method. the Kohn-Sham approach involves independent particles but an interacting density, an appreciation of which clarifies the way the method is used.

In the Kohn-Sham approach one replaces the difficult interacting many-body system being described the Hamiltonian (1.2) with a different auxiliary system that can be solved more easily. Since there is no unique prescription for choosing the simpler auxiliary system, this is an ansatz that rephrases the issues. The ansatz of Kohn and Sham assumes that the ground state density of the original interacting system is equal to that of some chosen non-interacting system that can be considered exactly soluble (in practice by numerical QMC scheme) with all the difficult many-body terms incorporated into an exchange-correlation functional of the density. By solving the equations one finds the ground state density and energy of the original interacting system with the accuracy limited only by the approximations in the exchange-correlation functional.

Indeed, the Kohn-Sham approach has led to very useful approximations that are now the basis of most calculations that attempt to make "first-principles" predictions for the properties of condensed matter and large molecular systems. The local density approximations (LDA) or various generalized-gradient approximations (GGA) are remarkably accurate, most notably for "wide-band" systems, such as the group II and II-IV semiconductors, sp-bounded metals like Na and Al, insulators like diamond, NaCl, and molecules with covalent and/or ionic bonding.

The Kohn-Sham construction of an auxiliary system based on two assumptions.
1. The exact ground state density can be represented by the ground state density of an auxiliary system of non-interacting particles. This is called "non-interacting-V-representability" ; although there are no rigorous proofs for real systems of interest, we will proceed assuming its validity.

2.The auxiliary Hamiltonian is chosen to have the usual kinetic operator and an effective local potential $V^{\sigma}_{eff}(\mathbf{r})$ acting on an electron of spin σ at point $\mathbf{r}$. The local form is not essential, but it is an extremely useful simplification that is often taken as the defining characteristic of the Kohn-Sham approach.

The actual calculations are performed on the auxiliary independent-particle system defined by the auxiliary Hamiltonian(using Hartee atomic units)

$$\hat{H}^{\sigma}_{aux} = -\frac{1}{2}\nabla^2 + V^{\sigma}(\mathbf{r}). \tag{2.7}$$

At this point the form of $V^{\sigma}(\mathbf{r})$ is not specified and the expressions must apply for all $V^{\sigma}(\mathbf{r})$ in some range, in order to define functionals for a range of densities. For a system of $N = N_{\uparrow} + N_{\downarrow}$ independent electrons obeying this Hamiltonian, the ground state has one electron in each of the N_{σ} orbitals $\psi^{\sigma}_i(\mathbf{r})$ with the lowest eigenvalues ϵ^{σ}_i of the Hamiltonian (2.7). The density of the auxiliary system is given by sums of squares of the orbitals for each spin

$$n(\mathbf{r}) = \sum_{\sigma} n(\mathbf{r},\sigma) = \sum_{\sigma}\sum_{i=1}^{N^{\sigma}} |\psi^{\sigma}_i(\mathbf{r})|^2, \tag{2.8}$$

the independent-particle kinetic energy T_s is given by

$$T_s = -\frac{1}{2}\sum_{\sigma}\sum_{i=1}^{N^{\sigma}} \langle\psi^{\sigma}_i|\nabla^2|\psi^{\sigma}_i\rangle = \frac{1}{2}\sum_{\sigma}\sum_{i=1}^{N^{\sigma}} \int d^3\mathbf{r}|\psi^{\sigma}_i(\mathbf{r})|^2, \tag{2.9}$$

and we define the classical Coulomb interaction energy of the electron density $n(\boldsymbol{r})$ interacting with itself

$$E_{Hartree}[n] = \frac{1}{2}\int d^3\mathbf{r}d^3\mathbf{r}'\frac{n(\mathbf{r})n(\mathbf{r}')}{|\mathbf{r}-\mathbf{r}'|}. \tag{2.10}$$

The Kohn-Sham approach to the full interacting many-body problem is to rewrite the Hohenberg-Kohn expression for the ground state energy functional in the form

$$E_{KS} = T_s[n] + \int d\mathbf{r}\, V_{ext}(\mathbf{r})n(\mathbf{r}) + E_{Hartree}[n] + E_{II} + E_{xc}[n]. \tag{2.11}$$

Here $V_{ext}(\mathbf{r})$ is the external potential due to the nuclei and other external fields(assumed to be independent of spins) and E_{II} is the interaction between the nuclei.

2.2. THE HOHENBERG-KOHN THEOREMS

Solution of the Kohn-Sham auxiliary system for the ground state can be viewed as the problem of minimization with respect to either the density $n(\mathbf{r},\sigma)$ or the effective potential $V^{\sigma}_{eff}(\mathbf{r})$. Since T_s is explicitly expressed as the functional of the orbitals but all other terms are considered to be functionals of the density, one can vary the wave functions and use the chain rule to derive the variational equation

$$\frac{\delta E_{KS}}{\delta\psi_i^{\sigma*}(\mathbf{r})} = \frac{\delta T_s}{\delta\psi_i^{\sigma*}(\mathbf{r})} + \left[\frac{\delta E_{ext}}{\delta n(\mathbf{r},\sigma)} + \frac{\delta E_{Hartree}}{\delta n(\mathbf{r},\sigma)} + \frac{\delta E_{xc}}{\delta n(\mathbf{r},\sigma)}\right]\frac{\delta n(\mathbf{r},\sigma)}{\delta\psi_i^{\sigma*}(\mathbf{r})} = 0, \quad (2.12)$$

subject to the orthonormalization constraints

$$\langle\psi_i^{\sigma}|\psi_j^{\sigma'}\rangle = \delta_{i,j}\delta_{\sigma,\sigma'}. \quad (2.13)$$

This is equivalent to the Rayleigh-Ritz principle [5, 6].
Using expressions (2.8) and (2.9) for $n^{\sigma}(\mathbf{r})$ and T_s, which give

$$\frac{\delta T_s}{\delta\psi_i^{\sigma*}(\mathbf{r})} = -\frac{1}{2}\nabla^2\psi_i^{\sigma}(\mathbf{r}); \frac{\delta n^{\sigma}(\mathbf{r})}{\delta\psi_i^{\sigma*}(\mathbf{r})} = \psi_i^{\sigma}(\mathbf{r}), \quad (2.14)$$

and the Lagrange multiplier method for handling the constraints:

$$\delta[\langle\Psi|\hat{H}|\Psi\rangle - E(\langle\Psi|\Psi\rangle - 1)] = 0$$
$$\langle\delta\Psi|\hat{H} - E|\Psi\rangle = 0$$

this leads to the Kohn-Sham Schrödinger-like equations:

$$(H^{\sigma}_{KS} - \varepsilon_i^{\sigma})\psi_i^{\sigma}(\mathbf{r}) = 0, \quad (2.15)$$

where the ε_i are the eigenvalues, and H^{σ}_{KS} is the effective Hamiltonian(in Hartree atomic units)

$$H^{\sigma}_{KS}(\mathbf{r}) = -\frac{1}{2}\nabla^2 + V^{\sigma}_{KS}(\mathbf{r}), \quad (2.16)$$

with

$$\begin{aligned} H^{\sigma}_{KS}(r) &= V_{ext}(\mathbf{r}) + \frac{\delta E_{Hartree}}{\delta n(\mathbf{r},\sigma)} + \frac{\delta E_{xc}}{\delta n(\mathbf{r},\sigma)} \\ &= V_{ext}(\mathbf{r}) + V_{Hartree}(\mathbf{r}) + V^{\sigma}_{xc}(\mathbf{r}). \end{aligned} \quad (2.17)$$

Equations (2.15)-(2.17) are well-known Kohn-Sham equations, with the resulting density $n(\mathbf{r},\sigma)$ and total energy E_{KS} given by (2.8) and (2.11). The equations have the form of independent-particle equations with a potential that must be found self-consistently with the resulting density. These equations are independent of any approximations to the functional $E_{xc}[n]$, and would lead to the exact ground state density and energy for the interacting system, if the exact functional $E_{xc}[n]$ were known.

2.3 LSDA approximation

Solids can be often be considered as close to the limit of the homogeneous electron gas. In that limit, it is known that effects of exchange and correlation are local in character, and local density approximation(or more generally the local spin density approximation (LSDA)), is reasonable, in which the exchange-correlation energy at each point assumed to be the same as in homogeneous electron gas with that density,

$$\begin{aligned} E_{xc}^{LSDA}[n^{\uparrow}, n^{\downarrow}] &= \int d^3\mathbf{r} n(\mathbf{r}) \epsilon_{xc}^{hom}(n^{\uparrow}(\mathbf{r}), n^{\downarrow}(\mathbf{r})) \\ &= \int d^3\mathbf{r} n(\mathbf{r}) [\epsilon_{x}^{hom}(n^{\uparrow}(\mathbf{r}), n^{\downarrow}(\mathbf{r})) + \epsilon_{c}^{hom}(n^{\uparrow}(\mathbf{r}), n^{\downarrow}(\mathbf{r}))]. \end{aligned} \tag{2.18}$$

The LSDA can be formulated in terms of either two spin densities $n^{\uparrow}(\mathbf{r})$ and $n^{\downarrow}(\mathbf{r})$, or the total density $n(\mathbf{r})$ and the fractional spin polarization $\zeta(\mathbf{r})$

$$\zeta(\mathbf{r}) = \frac{n^{\uparrow}(\mathbf{r}) - n^{\downarrow}(\mathbf{r})}{n(\mathbf{r})}. \tag{2.19}$$

The LSDA is the most general local approximation. For unpolarized systems the LDA is found simply by setting $n^{\uparrow}(\mathbf{r}) = n^{\downarrow}(\mathbf{r}) = n(\mathbf{r})/2$.

2.4 Linear Muffin-Tin Orbital (LMTO) formalism

The LMTO's calculation scheme [7] is based on the concept of muffin-tin potential which has proven to be a highly successful approximation of potential of realistic close-packed systems. In this concept the potential for a solid is approximated by a non-overlapping atomic-like spherical symmetric potential inside a sphere with radius S, and a constant in the interstitial region

$$V(r) = \begin{cases} V(|\boldsymbol{r}|), & r \leq \mathrm{S} \\ \\ V_{\mathrm{c}}, & r > \mathrm{S}. \end{cases} \tag{2.20}$$

Therefore, the Schrödinger equation can be solved exactly in both regions ($r \leq S$ and $r > S$). These solutions are matched at the sphere boundaries to produce the muffin-tin orbitals. To reduce the effect of interstitial region one introduces the overlapping atomic spheres which fill the whole volume of the crystal. In this, the so-called Atomic Sphere Approximation (ASA), the

volume of interstitial region equals to *zero*, i.e., the electron kinetic energy $\kappa^2 = \varepsilon - V_c$ in this region becomes a free parameter which can be taken equal to *zero*. In this case wave function inside a sphere (for $r \leq S$) satisfies to the radial Schrödinger equation, whereas outside it corresponds to the solution of Laplace equation $\nabla^2\Phi = 0$. Therefore, the radial part of the wave function can be written as

$$\Phi_l(r,\varepsilon) = \begin{cases} u_l(r,\varepsilon), & r \leq S \\ \left[\frac{D_l+l+1}{2l+1}(\frac{r}{S})^l + \frac{l-D_l}{2l+1}(\frac{r}{S})^{-l-1}\right] u_l(S,\varepsilon), & r > S, \end{cases} \tag{2.21}$$

where $u_l(r,\varepsilon)$ is the exact radial solution of Schrödinger equation which is normalized by one in the MTO sphere with radius S. These functions are not convenient to use as basis functions because of its divergence for large r. In order to construct decaying for large r, continuous and smooth in the whole space basis functions one has to substract the divergent wave $\frac{D_l+l+1}{2l+1}(\frac{r}{S})^l$ from both parts of (2.21)

$$\bar{\Phi}_l(r,D) = \begin{cases} \Phi(r,D) - \frac{D+l+1}{2l+1}\,\frac{\Phi_l(S,D)}{\Phi_l(S,l)}\,\Phi_l(r,l), & r \leq S \\ \frac{l-D}{2l+1}\,[\frac{r}{S}]^{-l-1}\,\Phi_l(S,D), & r > S, \end{cases} \tag{2.22}$$

where $D_L(\varepsilon)$ is the logarithmic derivative of the radial part of wave function at the sphere radius S

$$D_L(\varepsilon) = S\frac{\dot{u}_l(r,\varepsilon)}{u_l(r,\varepsilon)}\Big|_{r=S}. \tag{2.23}$$

The obtained functions are not (any more) the solutions of Schrödinger equation inside the atomic sphere. However, it is convenient to use them to built up the Bloch sums of the crystal. Taking into account all tails of basis functions from the other sites in central sphere at $\boldsymbol{R}_s$, the Bloch sums can be written as

$$\chi_L^{\boldsymbol{k}}(\boldsymbol{r},D) = \sum_{\boldsymbol{R}_s \neq 0} e^{i\boldsymbol{k}\cdot\boldsymbol{R}_s}\,\bar{\Phi}_L(\boldsymbol{r}-\boldsymbol{R}_s,D), \tag{2.24}$$

where tails from the center with radius-vector $\boldsymbol{R}_S$ are defined by

$$\bar{\Phi}_L(\boldsymbol{r}-\boldsymbol{R}_s,D) = i^l Y_L(\boldsymbol{r}-\boldsymbol{R}_s)\Big|\frac{\boldsymbol{r}-\boldsymbol{R}_s}{S}\Big|^{-l-1}\,\frac{l-D}{2l+1}\,\Phi_l(S,D). \tag{2.25}$$

Taking tails expansion in partial waves at the center of sphere and making the Bloch basis functions continuous and differentiable on the sphere surface,

one obtains

$$\chi_L^{\boldsymbol{k}}(\boldsymbol{r},D)=\begin{cases}\Phi_L(\boldsymbol{r},D)-\Phi_l(S,D)\,\frac{l-D}{2l+1}\,\sum_{L'}\Big[S^{\boldsymbol{k}}_{L'L}-\frac{D+l+1}{l-D}\times \\ \qquad\times 2(2l+1)\,\delta_{LL'}\Big]\,\frac{\Phi_{L'}(\boldsymbol{r},l')}{2(2l'+1)\,\Phi_{l'}(S,l')}, & r\le S,\\ \Phi_l(S,D)\,\frac{l-D}{2l+1}\Big[i^l Y_L(\boldsymbol{r})(\frac{r}{S})^{-l-1}+\sum_{L'}S^{\boldsymbol{k}}_{L'L}\times \\ \qquad\times i^{l'}Y_{L'}(\boldsymbol{r})(\frac{r}{S})^{l'}\frac{1}{2(2l'+1)}\Big], & r>S.\end{cases}\tag{2.26}$$

Here, $\chi_L^{\boldsymbol{k}}(\boldsymbol{r},D)$ are the so-called muffin-tin orbitals, and $S^{\boldsymbol{k}}_{L'L}$ are the structural constants which are defined via

$$\begin{aligned}S^{\boldsymbol{k}}_{LL'} &= \sum_{\boldsymbol{R}} e^{i\boldsymbol{k}\cdot\boldsymbol{R}}S^{\boldsymbol{R}}_{LL'},\ \text{and}\\ S^{\boldsymbol{R}}_{LL'} &= -\frac{8\pi(2l+2l'-1)!!}{(2l-1)!!(2l'-1)!!}\sum_{L''}C_{LL''L'}(-i)^{l''}\Big(\frac{R}{S}\Big)^{-l''-1}Y_{L''}(\boldsymbol{R})\end{aligned}\tag{2.27}$$

where $C_{LL''L'}$ are the Gaunt's coefficients. $Y_L(\boldsymbol{R})$ are the corresponding spherical harmonics. The solution of Schrödinger equation of the whole crystal is a linear combination of MT-orbitals

$$\Psi_{\boldsymbol{k}}(\boldsymbol{r})=\sum_L C_L(\boldsymbol{k})\sum_{R_s\neq 0}e^{i\boldsymbol{k}\cdot\boldsymbol{R}_S}\,\chi_L^{\boldsymbol{k}}(\boldsymbol{r}-\boldsymbol{R}_S,D_l(\varepsilon))\tag{2.28}$$

which must be exact solution of the radial Schrödinger equation inside of atomic spheres. According to this condition all tails from other sites and unphysical terms in MT-orbital, that is proportional to $[i^lY_L(\boldsymbol{r})\,r^l]$, have to eliminate each other inside of all atomic spheres, i.e., the second term in $\chi_L^{\boldsymbol{k}}(\boldsymbol{r},D)$ (Eq. 2.26) will turn to zero. This gives a set of linear homogeneous equations

$$\sum_L(S^{\boldsymbol{k}}_{LL'}-\delta_{LL'}P_l(\varepsilon))\,C_L(\boldsymbol{k})\bar{\Phi}_l(S,D_l)=0,\tag{2.29}$$

where the total information about crystal potential is included in the potential functions

$$P_l(\varepsilon)=2(2l+1)\,\frac{D_l(\varepsilon)+l+1}{D_l(\varepsilon)-l}.\tag{2.30}$$

The crystal structure information is contained in the structural constants $S^{\boldsymbol{k}}_{LL'}$ (Eq. 2.27). Therefore, the main problem of band structure calculations is to find eigenvalues and eigenvectors for single atomic sphere with spherically

symmetric potential and $\boldsymbol{k}$-dependent boundary conditions which appears from neighboring spheres. By construction the MTO basis set $\chi_L^{\boldsymbol{k}}(\boldsymbol{r}, D)$ is an energy dependent. This considerably complicates numerical evaluation of the secular equation whose solution defines the energy spectra of the system

$$\det||\langle\chi_L^{\boldsymbol{k}}(\boldsymbol{r}, D)|\hat{H} - \varepsilon\hat{O}|\chi_L^{\boldsymbol{k}}(\boldsymbol{r}, D)\rangle|| = 0. \tag{2.31}$$

Here, $\hat{H}$ and $\hat{O}$ are the Hamiltonian and overlap operators, respectively.

To resolve such a difficulty the linear MTO (LMTO) method was introduced which is based on the power expansion of the original MTO's up to the linear order in energy. The energy independent LMTO basis set provides a rapid convergence of the method. Taking into account only linear term in the Taylor expansion for the MTO basis wave function in an arbitrary energy point ε_ν one obtains

$$\Phi(r, D) = \Phi_\nu(r) + w(D)\dot{\Phi}_\nu(R). \tag{2.32}$$

Here, $\Phi_\nu(r)$ is the value of wave function at the energy point ε_ν, i.e. $\Phi_\nu(r) = u_l(\varepsilon_\nu, r)$. $\dot{\Phi}_\nu(r)$ is the energy derivative of the wave function at the expansion point $\dot{\Phi}_\nu(r) = \frac{\partial}{\partial\varepsilon}u_l(\varepsilon, r)|_{\varepsilon=\varepsilon_\nu}$ which is normalized by one in the atomic sphere with radius S. $w(D)$ is calculated as follows

$$w(D) = -\frac{\Phi_\nu(r)}{\dot{\Phi}_\nu(r)}\frac{D - D_\nu}{D - D_{\dot{\nu}}}, \tag{2.33}$$

where D is the logarithmic derivative on the atomic sphere surface

$$D = \frac{\Phi'(r, D)}{\Phi(r, D)}\Big|_{r=S.} \tag{2.34}$$

D_ν and $D_{\dot{\nu}}$ are defined via $D_\nu = S\frac{\Phi'_\nu(S)}{\Phi_\nu(S)}$ and $D_{\dot{\nu}} = S\frac{\dot{\Phi}'_\nu(S)}{\dot{\Phi}_\nu(S)}$, respectively.

The expansion energy point ε_ν is selected within the region of energies occupied by the valence electrons which is obtained from the solution of the Schrödinger equation within the atomic sphere. Therefore, if we consider an arbitrary energy ε, then the LMTO's have an error of order $(\varepsilon - \varepsilon_\nu)^2$ within the spheres.

In the LMTO basis set matrix elements of the Hamiltonian and overlap matrix inside of sphere can be written as

$$\begin{aligned}
&\langle\Phi'_L(D', S)|\hat{H} - \varepsilon_\nu\hat{O}|\Phi_L(D, S)\rangle = \delta_{L,L'}\, w_l(D), \\
&\langle\Phi'_L(D', S)|\Phi_L(D, S)\rangle = \delta_{L,L'}\,(1 + \langle\dot{\Phi}^2_{\nu l}|\Phi_L(D, S)\rangle w_l(D)w_l(D')),
\end{aligned} \tag{2.35}$$

where $\Phi_L(r,D)$ is orthogonal to $\dot{\Phi}_\nu(r)$ because of the normalization condition $\langle\Phi(r,\varepsilon)|\Phi(r,\varepsilon)\rangle = 1$ and $\frac{\partial}{\partial\varepsilon}\langle\Phi(r,\varepsilon)|\Phi(r,\varepsilon)\rangle = 2\langle\dot{\Phi}(r,\varepsilon)|\Phi(r,\varepsilon)\rangle = 0$.

The Hamiltonian Eq.(2.36) describes a single atomic sphere. In order to build up a crystal where each sphere affects to the energy spectra one introduces a set of potential parameters $w_l(D_1)$, $S\Phi^2(D_1), \Phi^2(D_1)/\Phi^2(D_2)$ with $D_1 = -l-1$ and $D_2 = l$. Using these potential parameters the basis orbitals $\chi^{\boldsymbol{k}}_L(\boldsymbol{r},D)$ can be written as

$$\chi^{\boldsymbol{k}}_L(\boldsymbol{r},D) = \frac{w_l(l)-w_l(D)}{w_l(l)-w_l(-l-1)}\chi^{\boldsymbol{k}}_L(\boldsymbol{r}) = \alpha_l(D)\chi^{\boldsymbol{k}}_L(\boldsymbol{r}), \tag{2.36}$$

where $\chi^{\boldsymbol{k}}_L(\boldsymbol{r})$ is defined according to

$$\chi^{\boldsymbol{k}}_L(\boldsymbol{r}) = \Phi_L(\boldsymbol{r},-l-1) - \Phi_l(S,-l-1)\sum_{L'} S^{\boldsymbol{k}}_{L'L}\frac{\Phi'_L(\boldsymbol{r},l')}{2(2l'+1)\Phi'_l(S,l')} \tag{2.37}$$

The Hamiltonian and overlap matrix of the crystal are

$$\begin{aligned} H^{\boldsymbol{k}}_{L'L} &= \langle\chi^{\boldsymbol{k}}_{L'}(\boldsymbol{r})|\hat{H}|\chi^{\boldsymbol{k}}_L(\boldsymbol{r})\rangle = H^{(1)}_{l'}\delta_{L'L} + \Big[-(H^{(2)}_{l'}+H^{(2)}_l)S^{\boldsymbol{k}}_{L'L} + \\ &+ \sum_{L''} S^{\boldsymbol{k}}_{L'L''}H^{(3)}_{L''}S^{\boldsymbol{k}}_{L''L}\Big]\frac{S}{2}\Phi_{l'}(S,-l'-1)\Phi_l(S,-l-1), \\ O^{\boldsymbol{k}}_{L'L} &= \langle\chi^{\boldsymbol{k}}_{L'}(\boldsymbol{r})|\chi^{\boldsymbol{k}}_L(\boldsymbol{r})\rangle = O^{(1)}_{l'}\delta_{L'L} + \Big[-(O^{(2)}_{l'}+O^{(2)}_l)S^{\boldsymbol{k}}_{L'L} + \\ &+ \sum_{L''} S^{\boldsymbol{k}}_{L'L''}O^{(3)}_{L''}S^{\boldsymbol{k}}_{L''L}\Big]\frac{S}{2}\Phi_{l'}(S,-l'-1)\Phi_l(S,-l-1), \end{aligned} \tag{2.38}$$

with

$$\begin{aligned} O^{(1)}_l &= 1 + \langle\dot{\Phi}^2_{\nu l}\rangle w^2_l(-l-1); \\ O^{(2)}_l &= \frac{1+\langle\dot{\Phi}^2_{\nu l}\rangle w_l(-l-1)w_l(l)}{w_l(-l-1)-w_l(l)}; \\ O^{(3)}_l &= \frac{1+\langle\dot{\Phi}^2_{\nu l}\rangle w^2_l(l)}{2S[(2l+1)\Phi_l(S,l)]^2}; \\ H^{(1)}_l &= w_l(-l-1) + \varepsilon_{\nu l}O^{(1)}_l; \\ H^{(2)}_l &= \frac{1}{2}\frac{w_l(l)}{w_l(-l-1)-w_l(l)} + \varepsilon_{\nu l}O^{(2)}_l; \\ H^{(3)}_l &= \frac{w_l(l)}{2S[(2l+1)\Phi_l(S,l)]^2} + \varepsilon_{\nu l}O^{(3)}_l, \end{aligned} \tag{2.39}$$

where $H^{(1)}$, $H^{(2)}$, and $H^{(3)}$ terms can be treated like one-, two-, and three-centers integrals respectively.

Chapter 3

Dynamical Mean-Field Theory

The dynamical mean-field theory can be obtained in many ways [8], which differ between each other for the mathematical formalism adopted and the degree of complexity. The most pedagogical derivation starts probably from a comparison with the Weiss molecular field theory for the Ising model.

The Ising model is a lattice of classical spins S_i described by the Hamiltonian

$$H = -J \sum_{i,j} S_i S_j - h \sum_i S_i, \tag{3.1}$$

where h is the energy of single spin in an external(magnetic) field and J is the ferromagnetic energy due to a spin-spin interaction. To keep the model realistic the first sum is limited to indexes that run for pairs of nearest neighbors. The presence of the interaction term correlates the spin between each other. which makes the system hard to solve directly. However, if we focus on one physical quantity, we can try to reduce it to a simpler equivalent system that we are able to solve. Let us focus on the magnetization at site i

$$m_i \equiv \langle S_i \rangle, \tag{3.2}$$

the is the thermal average of a spin at a single site. Our equivalent system is a lattice of non-interacting spins moving in an effective site-dependent field h^{eff} and the corresponding Hamiltonian is

$$H_{eff} = -\sum_i h_i^{eff} S_i. \tag{3.3}$$

The effective field should be chosen to reproduce the same magnetization m_i of the original lattice. Calculating the sum over all the possible configurations for (3.3), we can write down an explicit expression for the effective field:

$$\beta h_i^{eff} = tanh^{-1} m_i, \tag{3.4}$$

where $\beta = 1/k_B T$. Up to now we have not made any approximations, but we still have not obtained a relation with the original system. In the Weiss mean-field theory the effective field is approximated by the thermal average of the local field seen by a spin at a given site:

$$h_i^{eff} \simeq h + J \sum_j \langle S_i \rangle = h + Jzm_i. \tag{3.5}$$

In the last step we have contextualized our discussion to a translational invariant system with z nearest neighbors for every site. The equation (3.4) and (3.5) can be solved analytically, leading to the approximated magnetization. We have to stress that the procedure of the mapping into an equivalent non-interacting system is exact with respect to the chosen observable: the approximation is made when establishing a relation between the Weiss field and the neighboring sites. Furthermore the approximation becomes exact in the limit of $z \to \infty$ [9]. This result is quite intuitive: the neighbors of a given site can be globally treated as bath when their number becomes large.

All these ideas can be easily extended to the Hubbard model [10]. Being a fully-interacting quantum many-body system, the mapping procedure is not as obvious as above, but can be established on rigorous basis. For simplicity we consider the one-band Hubbard model [11, 12, 13]

$$\hat{H}_{hub} = -t \sum_{\mathbf{R},\mathbf{R}'} \hat{c}^+_{\mathbf{R},\sigma} \hat{c}_{\mathbf{R}',\sigma} + U \sum_{\mathbf{R}} n_{\mathbf{R},\uparrow} n_{\mathbf{R},\downarrow}. \tag{3.6}$$

Instead of the magnetization, we focus on the local Green's function at a single site:

$$G^{\sigma}_{\mathbf{R},\mathbf{R}'}(\tau - \tau') \equiv -\langle T \hat{c}_{\boldsymbol{R},\sigma}(\tau) \hat{c}^+_{\boldsymbol{R}',\sigma}(\tau') \rangle. \tag{3.7}$$

Here τ and τ' are imaginary times in the Matsubara's formalism for the perturbation theory at finite temperature and T is the time-ordering operator.

As before, we would like to chose the reference system as a single site embedded in an effective field. Since the Green's function (3.7) is time dependent, the new field must also evolve in time, i.e. must be dynamical. The simplest field we can imagine is a bath of non-interacting electrons. The single site, the bath and their coupling can be described by the following Hamiltonian:

$$\hat{H}_{eff} = \hat{H}_{atom} + \hat{H}_{bath} + \hat{H}_{coupling}. \tag{3.8}$$

The first term

$$\hat{H}_{atom} = U \hat{c}^+_{\uparrow} \hat{c}_{\uparrow} \hat{c}^+_{\downarrow} \hat{c}_{\downarrow} \tag{3.9}$$

is the Coulomb repulsion of two electrons at the atomic site, and $\hat{c}$, $\hat{c}^+$ are the corresponding spin-dependent annihilation and creation operators. Notice

that this term comes directly from the initial equation (3.6). To assure a formal distinction between the operators of the original model and the lattice model we have omitted the index $\boldsymbol{R}$. The second term of the equation (3.8) is

$$\hat{H}_{bath} = \sum_{k,\sigma} \varepsilon_{k,\sigma} \hat{a}^{+}_{k,\sigma} \hat{a}_{k,\sigma} \tag{3.10}$$

and represents the fictitious sea of electrons whose quantum numbers are their spin σ and number of site in the bath k. We use $\hat{a}$ and $\hat{a}^{+}$ for the corresponding annihilation and creation operators, and $\varepsilon_{k,\sigma}$ for the bath orbital energies. Finally the last term of equation (3.8)

$$\hat{H}_{coupling} = \sum_{k,\sigma} V_{k,\sigma} (\hat{a}^{+}_{k,\sigma} \hat{c}_{\sigma} + \hat{c}^{+}_{\sigma} \hat{a}_{k,\sigma}), \tag{3.11}$$

describes the exchange of electrons between site and bath at an energy $\varepsilon_{k,\sigma}$ with amplitude $V_{k,\sigma}$.

The Hamiltonian (3.8) is a well-known problem in many-body physics: it is a single impurity Anderson model . In the last 40 years it has been studied extensively and nowadays can be solved through many methods, depending on the range of the parameters and on the allowed approximations . By now we are interested in finding the connection of the parameters $\varepsilon_{k,\sigma}$ and $V_{k,\sigma}$ with the full solution of the problem, i.e. the analogous formula to equation (3.4). To this aim we treat the first term of equation (3.8) as a perturbation [14]; then the other two terms determine the unperturbed Green's function of the bath G_0. Passing from the imaginary time τ to the Matsubara frequencies $i\omega_i$, we have

$$G^{\sigma}_{0}(i\omega_n) = \frac{1}{i\omega_n + \mu - \Delta^{\sigma}(i\omega_n)} \tag{3.12}$$

where μ is the chemical potential, which sets the correct number of particles, and the quantity

$$\Delta^{\sigma}(i\omega_n) = \sum_{k} \frac{|V_{k,\sigma}|^2}{i\omega_n - \varepsilon_k} \tag{3.13}$$

is called hybridization function. In terms of many-body perturbation theory the full Green's function of the Hamiltonian (3.8) can be obtained by means of the Dyson equation

$$G^{\sigma}_{imp} = [G^{\sigma}_{0}(i\omega_n)^{-1} - \Sigma^{\sigma}_{imp}(i\omega_n)]^{-1}, \tag{3.14}$$

where Σ_{imp} is the self-energy function and contains all the effects of the interactions. Σ_{imp} depends only on the unperturbed Green's function G_0 and the interaction term equation (3.9). The parameters $\varepsilon_{k,\sigma}$ and $V_{k,\sigma}$ enter

in the full problem only through G_0, which takes the meaning of the "Weiss" field and which is determined to have the impurity full Green's function (3.14) coincide with the local Green's function (3.7):

$$G^{\sigma}_{imp}(i\omega_n) = G^{\sigma}_{R,R'}(i\omega_n). \tag{3.15}$$

The fact the parameters do not appear explicitly in the mapping procedure makes it more rigorous to redefine the problem in terms of an effective action formalism [15], instead of the Hamiltonian (3.8). Integrating out the bath degrees of freedom, we can write down the effective action for the orbital of the impurity as

$$S = -\int_0^{\beta} d\tau \int_0^{\beta} d\tau' \sum_{\sigma} \hat{c}^{+}_{\sigma}(\tau)[G^{\sigma}_0(\tau-\tau')]^{-1}\hat{c}_{\sigma}(\tau') + U\int_0^{\beta} d\tau\, \hat{c}^{+}_{\uparrow}(\tau)\hat{c}_{\uparrow}(\tau)\hat{c}^{+}_{\downarrow}(\tau)\hat{c}_{\downarrow}(\tau). \tag{3.16}$$

The action S fully determines the dynamics of the local site under consideration: the first term takes into account electrons jumping from the bath on the site at τ and coming back to the bath at τ'; the second term includes the Coulomb repulsion when two electrons with opposite spins are present on the site at the same time. Now we have the most rigorous expression for the full Green's function of the impurity:

$$G^{\sigma}_{imp}(\tau-\tau') \equiv -\langle T\hat{c}_{\sigma}(\tau)\hat{c}^{+}_{\sigma}(\tau')\rangle_S. \tag{3.17}$$

Anyway we must stress again that in both the formulations in terms of Dyson's equation or in terms of the effective action, the central point is the preservation relation (3.15).

Up to now the representation of the chosen observable of the original lattice is exact. The approximation is done with the next step: the connection of the two systems. In the DMFT the lattice self-energy is only local and coincides with the self-energy of the impurity model:

$$\Sigma^{\sigma}_{R,R'}(i\omega_n) = \delta_{R,R'}\Sigma^{\sigma}_{imp}(i\omega_n). \tag{3.18}$$

In the reciprocal space it means that the self-energy becomes k-independent.

While the approximation (3.18) can appear rather arbitrary,indeed is mathematically very similar to equation (3.5). In fact it becomes exact in the limit of infinite nearest neighboring sites, or equivalently, infinite dimensions, as was proved by Metzer and Vollhardt in a work [16] that is considered the first mile-stone of the DMFT. One year later, George and Kotliar [9] completed the main framework of the theory by proving that in the same limit the

Hubbard model can be exactly mapped into the Anderson impurity model. Their proof is based on the fact that the topology of all irreducible Feynman diagrams becomes the same in the two systems: simply the local contribution of all the diagrams. The parallelism between the Weiss mean-field theory for the classical Ising model and the quantum Hubbard model is summarized in Table 3. In addition we show also that the same representation can be constructed for the Kohn-Sham equations. In this case the original system is the many-electron Hamiltonian (1.2), and the mapping system is the non-interacting electron gas (2.16) in the effective potential V_{KS}. The approximation comes with the LDA exchange-correlation functional (2.18). It is clear that a strong mathematical connection exists between these generalized mean-field theories. More precisely all the three of them can be seen as generalization of the thermodynamical Legendre transformation

Before ending the Chapter we should emphasize that the convergence of the DMFT approximation with respect to the number of neighbors is very fast, and this makes it applicable also for more realistic cases, like a 3-dimensional solid. Moreover there are two other limits for which the DMFT becomes exact:

- in the atomic limit $t = 0$ the sites are decoupled from each other, so that the hybridization function $\Delta(i\omega_n)$ is zero; as a result the self-energy has only on-site component, i.e. it is local
- in the non-interacting limit $U = 0$ the self-energy becomes zero, and then again trivially local.

Original System	Ising Model	Hubbard Model	Electron Hamiltonian
Mapping System	Spins in a Effective Field	Single Impurity Anderson Model	Electrons in an Effective Potentail
Selected Observable	Magnetization m_i	Green's Function $G_{R,R'}(\tau - \tau')$	Electron Dencity $n(r)$
Approximation	$h_i^{eff} \simeq h + zZm_i$	$\Sigma^{\sigma}_{R,R'} \simeq \delta_{R,R'}\Sigma^{\sigma}_{imp}$	$E_{xc}[n] \simeq E_{xc}^{LDA}[n]$

3.1 Exact Diagonalization

Exact diagonalization methods are important tools for studying the physical properties of quantum many-body systems. These methods typically are used to determine a few of the lowest eigenvalues and eigenvectors of models of many-body systems on a finite lattice. From these eigenvalues and eigenvectors, various ground state expectation values and correlation functions are easily computed. Although the methods are limited to small lattice

sizes, they have become increasingly popular because of using with DMFT. In addition to provideng useful benchmarks for approximate theoretical calculations and quantum Monte Carlo simulations they help to provide insight into the often subtle properties of unsolvable many-body problems in the thermodynamical limit.

The expression "Exact diagonalization" is used to describe a number of different approaches [8, 17] which yield numerically exact results for a finite lattice system by directly diagonalizing the matrix representation of the system's Hamiltonian in an appropriate many-particle basis. The simplest, and the most time- and memory- consuming approach is the *exact diagonalization* [18, 19] of the matrix which enables one to calculate all desired properties. However, the dimension of the basis for a strongly interacting quantum systems grows exponentially with the system size, so it is impossible to treat systems with more than a few sites. If only properties of low- or high-lying eigenstates are required, (in the investigation of condensed matter systems one is often interested in the low-energy properties), it is possible to reach substantially larger system sizes using iterative diagonalization procedures, which also yields result to almost machine precision in most cases. The iterative diagonalization methods allow for the calculation of ground state properties and (with some extra efforts) some low-lying excited states are also accessible. In addition, it is possible to calculate dynamical properties (e.g. spectral functions, time evaluation) as well as behavior a finite temperature. Nearly every system and observable can be calculated in principle, although the convergence properties may depend on the system under investigation. In chapter 4 we will describe such iterative method - the Lanczos algorithm - in details.

3.2 Quantum Monte Carlo method. Hyrsch-Fye algorithm

The quantum Monte Carlo scheme is the most universal tool [20, 21] for the numerically study of quantum many-body systems with strong correlations. The auxiliary-field scheme allows to deal with fermionic systems with strong electronic correlations. The determinantal auxiliary-field algorithm, namely Hirsch-Fye appeared more than 20 years ago and became nowadays standard for the numerical investigation [22, 23] of physical models with with strong interactions, as well as for the quantum chemistry and nanoelectronics. We regard this method as it is an efficient as impurity solver within DMFT ,i.e. in solving Anderson impurity model.

3.2. QUANTUM MONTE CARLO METHOD. HYRSCH-FYE ALGORITHM

The one band single-impurity model is specified by the imaginary time effective action:

$$\begin{aligned} S_{eff} = &- \int_0^\beta d\tau d\tau' \sum_\sigma c_\sigma^+(\tau) G_\sigma^{-1}(\tau - \tau') c_\sigma(\tau') \\ &+ \int_0^\beta d\tau U n_\uparrow(\tau) n_\downarrow(\tau'), \end{aligned} \tag{3.19}$$

$$G_\sigma^{-1}(i\omega) = i\omega + \mu - \Delta_\sigma(i\omega), \tag{3.20}$$

where $c_\sigma^+(\tau)$ and $c_\sigma(\tau)$ are Grassmann variables, μ denotes the chemical potential, U is on-site Coulomb repulsion and $\Delta_\sigma(i\omega)$ is a hybridization function that describes transitions into the bath and back.

The aim of the impurity solver is to compute the Green's function

$$G(\tau - \tau') = \langle T_\tau c_\sigma^+(\tau) c_\sigma(\tau') \rangle_{S_{eff}} = \frac{Tr[T_\tau e^{-S_{eff}} c_\sigma^+(\tau) c_\sigma(\tau')]}{Tr[T_\tau e^{S_{eff}}]} \tag{3.21}$$

for a given hybridization function.

The first step in Hirsch-Fye algorithm is a discretization of the impurity model effective action (3.19):

$$S_{eff} \to \sum_{\tau\tau'\sigma} c_\sigma^+(\tau) G_\sigma^{-1}(\tau - \tau') c_\sigma(\tau') + U n_\uparrow(\tau) n_\downarrow(\tau'), \tag{3.22}$$

where the imaginary time is discretized in L "slices" $\tau = 1, 2, \ldots, L$ of size $\Delta\tau$, and the time step $\Delta\tau$ is defined by $\beta = L\Delta\tau$.

We temporarily introduce the Hamiltonian description of the local impurity problem, which permits a local in time description of the partition function. In order to preserve the standard notations for this model, the impurity orbital will be taken as a d orbital. The conduction bath orbitals are numbered from $p = 2, \ldots, n_s$, and the impurity orbitals is equivalently denoted by $c_{1\sigma} \equiv d_\sigma$, i.e. corresponds to $p = 1$. The Hamiltonian of a general Anderson impurity model reads

$$\begin{aligned} H = &\sum_{p\geq 2,\sigma} \varepsilon_p c_{p\sigma}^+ c_{p\sigma} + \sum_{p\geq 2,\sigma} V_p (c_{p\sigma}^+ d_\sigma + d_\sigma^+ c_{p\sigma}) \\ &\varepsilon_d \sum_\sigma d_\sigma^+ d_\sigma + U n_{d\uparrow} n_{d\downarrow} \end{aligned} \tag{3.23}$$

It is written as a sum of terms $H = H^0 + H^i$, where H^0 is a quadratic in the fermion operators:

$$\begin{aligned} H^0 \equiv &\sum_{p\geq 2,\sigma} \varepsilon_p c_{p\sigma}^+ c_{p\sigma} + \sum_{p\geq 2,\sigma} V_p (c_{p\sigma}^+ d_\sigma + d_\sigma^+ c_{p\sigma}) \\ &+ (\varepsilon_d + U/2) \sum_\sigma n_{d\sigma}, \end{aligned} \tag{3.24}$$

whereas H^i is a interaction term :

$$H^i \equiv U[n_{d\uparrow} n_{d\downarrow} - \frac{1}{2}(n_{d\uparrow} + n_{d\downarrow})]. \tag{3.25}$$

The discretization allows to write a partition function as

$$Z = Tr \prod_{l=1}^{L} e^{-\beta H} = Tr e^{-\Delta\tau[H^0 + H^i]} \tag{3.26}$$

The follow derivation is based on the Trotter-Suzuki transformation, namely for operators A and B

$$e^{(A+B)} = \lim_{L\to\infty} (e^{A/L} e^{B/L}) \tag{3.27}$$

This implies that $exp(-\Delta\tau(A+B)) = \lim_{\Delta\to 0} exp(-\Delta\tau A) exp(-\Delta\tau B) + O(\Delta\tau^2)$. Hence the exponential of the Hamiltonian in (3.26) is approximately factorized into Gaussian and interacting parts up to an error of order $O(\Delta\tau^2)$ by discretizing the imaginary time interval into L slices:

$$Z \simeq Z^{\Delta\tau} \equiv Tr \prod_{l=1}^{L} e^{-\Delta\tau H^0} e^{-\Delta\tau H^{int}} \tag{3.28}$$

The Green's function corresponding to Z^{Δ} can be defined analogously, by using $U_{\Delta\tau} \equiv exp(-\Delta\tau H^0) exp(-\Delta\tau H^i)$ and an evolution operator between time slices:

$$\begin{aligned} g^{\Delta\tau}_{p_1,p_2}(\tau_{l_1}, \tau_{l_2}) &\equiv \langle a_{p_1}(\tau_{l_1}) a^+_{p_2}(\tau_{l_2}) \rangle \\ &= \frac{Tr U^{L-l_1}_{\Delta\tau} a_{p_1}(\tau_{l_1}) U^{l_1-l_2}_{\Delta\tau} a^+_{p_2}(\tau_{l_2}) U^{l_2}_{\Delta\tau}}{Tr U^{L}_{\Delta\tau}}, \end{aligned} \tag{3.29}$$

we $l_1 > l_2$ is supposed.

The partition function is further evaluated by transforming the interacting problem into a noninteracting one. This happens at the cost of introducing auxiliary degrees of freedom and is facilitated by a discrete Hubbard-Stratonovich transformation [24, 25, 26], applied on each slices:

$$\begin{aligned} exp[-\Delta\tau H^i] =& \frac{1}{2} \sum_{s=\pm 1} exp[\lambda s (n_{d\uparrow} - n_{d\downarrow})], \\ & \cosh(\lambda) \equiv exp(\Delta\tau U/2) \end{aligned} \tag{3.30}$$

and after inserting (3.30) into (3.28), the partition function Z^{Δ} is reduced to

$$Z^{\Delta} = \frac{1}{2^L} \sum_{s_1,\ldots,s_L=\pm 1} Z^{\Delta}_{s_1,\ldots,s_L} = \frac{1}{2^L} \sum_{s_1,\ldots,s_L=\pm 1} \det O^{\uparrow}(\{S\} \det O^{\downarrow}(\{S\}) \quad (3.31)$$

with

$$Z^{\Delta}_{s_1,\ldots,s_L} = \prod_{\sigma=\pm 1(=\uparrow\downarrow)} Tre^{-\Delta\tau H^0} e^{V^{\sigma}(s_1)} \times e^{-\Delta\tau H^0} e^{V^{\sigma}(s_2)} \cdots e^{-\Delta\tau H^0} e^{V^{\sigma}(s_L)} \quad (3.32)$$

In equation (3.32), the $n_s \times n_s$ matrix $V^{\sigma}(s)$ is diagonal with

$$e^{V^{\sigma}(s)} = \begin{pmatrix} e^{\lambda\sigma s} & \cdots & \cdots & 0 \\ \cdots & 1 & \cdots & \cdots \\ \cdots & \cdots & 1 & \cdots \\ \cdots & \cdots & \cdots & 1 \end{pmatrix} \quad (3.33)$$

The matrices $O^{\sigma}(\{S\}$ have dimensions $N_s L \times N_s L$ and depend on the particular configuration of the Ising spins denoted by $\{S\}$.

The crucial fact noted by Hirsch and Fye is that the Green's functions for two different Ising spins configurations, $(s_1, \ldots, s_L)$ and $(s'_1, \ldots, s'_L)$, are related to each other by a Dyson equation. Abbreviating $g \equiv g^{\Delta\tau}_{s_1,\ldots,s_L}$ and $g' \equiv g^{\Delta\tau}_{s'_1,\ldots,s'_L}$, etc, this Dyson equation reads

$$g' = g + (g-1)(e^{V'-V} - 1)g'. \quad (3.34)$$

In fact, Eq. (3.34) relates two Green's functions g and g' via a projection operator on the d site, namely $[exp(V' - V) - 1]$. The presence of this projection operator comes from the possibility of the integrating out the conduction band. As a consequence, the Dyson equation (3.34) directly relates the Green's functions on the d site one to another, and this equation remains equally valid in the subspace $i_s = 1, i'_s = 1$. Hence, the d site Green's functions $G^{\Delta\tau}_{s_1,\ldots,s_L}$ also satisfy

$$G' = G + (G-1)(e^{V'-V} - 1)G', \quad (3.35)$$

viewed as an $L \times L$ matrix equation.

Rearranging Eq. (3.35), it is straightforward to see that $G_{s'_1,\ldots,s'_L}$ for an Ising configuration $(s'_1, \ldots, s'_L)$ can be obtained from $G_{s_1,\ldots,s_L}$ by inversion of an $L \times L$ matrix A, defined in the following equation

$$AG' = G, A \equiv 1 + (1 - G)[e^{V'-V} - 1]. \quad (3.36)$$

In the special case in which $(s'_1, \ldots, s'_L)$ differs from $(s'_1, \ldots, s'_L)$ by the value of a single spin, say s_l, A takes on a special form

$$A = \begin{pmatrix} 1 & 0 & A_{1l} & 0 & \cdots \\ 0 & 1 & A_{2l} & 0 & \cdots \\ \cdots & 0 & A_{ll} & \cdots & \cdots \\ \cdots & \cdots & \cdots & 1 & 0 \\ \cdots & \cdots & A_{Ll} & 0 & 1 \end{pmatrix} \tag{3.37}$$

In that case, $\det A = A_{ll} = 1 + (1 - G_{ll})[exp(V'_l - V_l) - 1]$. Expanding A^{-1} in minors, it can be easily be seen that $A^{-1}_{lk} = 0$ for $k \neq l$. In that case Eq. (3.36) simplifies to

$$G'_{l_1 l_2} = G_{l_1 l_2} + (G - 1)_{l_1 l}(e_{ll}^{V'-V} - 1)(A_{ll})^{-1} G_{l l_2}, \tag{3.38}$$

which is a special case of a Sherman-Morrison formula [27]. equation (3.34) can be also be used to show that

$$\begin{aligned} \frac{\det O'}{\det O} &= \frac{\det G}{\det G'} \\ &= \det A = 1 + (1 - G_{ll})[exp(V' - V) - 1] \end{aligned} \tag{3.39}$$

It is remarkable that all the equations (3.35-3.39) express exact relations between discretized Green's functions $G^{\Delta\tau}$. The only error left is related to the Trotter-Suzuki decomposition.

Chapter 4

Finite Temperature Lanczos Method

As was mentioned above the key quantity on which DMFT focuses is the local Green's function. In the case of finite temperatures it is defined on imaginary time as follows [28]

$$G_{ij}(\tau) = -\langle c_i(\tau) c_j^+(0)\rangle = -\frac{1}{Z} Tr\{e^{-\beta\hat{H}} c_i(\tau) c_j^+(0)\}, \tag{4.1}$$

where τ is imaginary time, $c_i^+(\tau)$, $c_i(\tau)$ are creation and annihilation operators acting on site with number i and defined in Heisenberg representation, β is inverse temperature and average is evaluated on grand canonical ensemble.

One of the advantages of Lanczos method is the capability to calculate Green's function on the real energies. It is due that the calculation is based on the Lehmann representation of the Green's function. We evaluate this formula due to Mahan [29]. Using eigenvalues and eigenstates for the system with Hamiltonian $\hat{H}$:

$$\hat{H}|\nu\rangle = E_\nu|\nu\rangle \tag{4.2}$$

the expression for Green's function reads

$$G_{ij}(\tau) = -\frac{1}{Z}\sum_\nu \langle\nu|e^{-\beta\hat{H}} c_i(\tau) c_j^+(0)|\nu\rangle,$$

where Z is a partition function:

$$Z = \sum_\nu e^{-\beta E_\nu} \tag{4.3}$$

Introducing the unit operator

$$\hat{1} = \sum_{\nu} |\nu\rangle\langle\nu|$$

and remember the transformation from Schrödinger to Heisenberg representation

$$\hat{c}_i(\tau) = e^{\tau\hat{H}}\hat{c}_i e^{-\tau\hat{H}} \tag{4.4}$$

it yields

$$\begin{aligned} G_{ij}(\tau) = -\frac{1}{Z}\sum_{\mu,\nu} e^{-\beta E_\nu}\langle\nu|c_i(\tau)|\mu\rangle\langle\mu|c_j^+(0)|\nu\rangle = \\ -\frac{1}{Z}\sum_{\mu,\nu} e^{-\beta E_\nu}\langle\nu|e^{\tau\hat{H}}c_i\, e^{-\tau\hat{H}}|\mu\rangle\langle\mu|c_j^+|\nu\rangle = \\ -\frac{1}{Z}\sum_{\mu,\nu} e^{-\beta E_\nu}e^{-\tau(E_\nu-E_\mu)}\langle\nu|c_i\,|\mu\rangle\langle\mu|c_j^+|\nu\rangle \end{aligned}$$

To obtain Green's function on energy scale one needs to apply the Fourier transformation

$$G_{ij}(i\omega_n) = \int_0^\beta G_{ij}(\tau)e^{i\omega_n}\, d\tau \tag{4.5}$$

$$\begin{aligned} G_{ij}(i\omega_n) = -\frac{1}{Z}\sum_{\mu,\nu}\langle\nu|c_i|\mu\rangle\langle\mu|c_j^+|\nu\rangle e^{-\beta E_\nu}\int_0^\beta d\tau\, e^{\tau(i\omega_n+E_\nu-E_\mu)} = \\ -\frac{1}{Z}\sum_{\mu,\nu}\langle\nu|c_i|\mu\rangle\langle\mu|c_j^+|\nu\rangle e^{-\beta E_\nu}\,\frac{e^{i\beta\omega_n}\cdot e^{\beta(E_\nu-E_\mu)}-1}{i\omega_n+E_\nu-E_\mu} \end{aligned}$$

and with $\omega_n = \frac{(2n+1)\pi}{\beta}$ called Matsubara frequencies, $e^{i\omega_n\beta} = -1$ for fermions

$$\begin{aligned} G_{ij}(i\omega_n) = -\frac{1}{Z}\sum_{\mu,\nu}\langle\nu|c_i|\mu\rangle\langle\mu|c_j^+|\nu\rangle e^{-\beta E_\nu}\,\frac{(-1)\cdot e^{\beta(E_\nu-E_\mu)}-1}{i\omega_n+E_\nu-E_\mu} = \\ \frac{1}{Z}\sum_{\mu,\nu}\frac{\langle\nu|c_i|\mu\rangle\langle\mu|c_j^+|\nu\rangle}{i\omega_n+E_\nu-E_\mu}\Big[exp(-\beta E_\mu)+exp(-\beta E_\nu)\Big] \end{aligned} \tag{4.6}$$

This Green's function is well defined i.e. has no singularities on imaginary axis [30]. Therefore it is suitable as a quantity to be self-consistent within DMFT iterations. But physical properties, for instance the density of states is expressed through Green's function on real energies. The retarded Green's function on real energies could be obtained in the same manner as the Green's function on imaginary time. One can see that the former is an analytical continuation of the latter with $i\omega_n \to E + i\delta$ substitution [29].

$$G_{ij}^{Ret}(E) = \frac{1}{Z}\sum_{\mu,\nu}\frac{\langle\nu|c_i|\mu\rangle\langle\mu|c_j^+|\nu\rangle}{E + i\delta + E_\nu - E_\mu}\left[exp(-\beta E_\mu) + exp(-\beta E_\nu)\right] \qquad (4.7)$$

The direct usage of (4.7) leads to full exact diagonalization method. However, this method has at least two problems. At the beginning it requires the full solution of eigenproblem. It is a high memory consuming process. In terms of Anderson impurity model(AIM) only values of n_s of the order $n_s = 7$ [which leads to the diagonalization of a 1225x1225 matrix in the sector $(n^\uparrow = 4, n^\downarrow = 3)$] or $n_s = 8$ (4900x4900) is reachable. If an impurity site in AIM represents transition element with five orbitals then one could add only three bath orbitals. That does not allow to much. It is more disappointed if only low energy states are reasonable in the case of low temperature.

Then one has to evaluate Green's function due to (4.6) or (4.7). There are several problems with it from the point of view of float point mathematics. The main problem is that this expression is very sensitive to errors in eigenenergies E_ν and eigenstates $|\nu\rangle$. The other one that is no evidence how much terms in (4.6) one has to take into account to reach enough accuracy. That is because the sum over eigenstates is not monotonic. Introducing some notations for convenience

$$G^\xi(E) = \frac{1}{Z}\sum_{\mu,\nu<\xi}\frac{\langle\nu|c_i|\mu\rangle\langle\mu|c_j^+|\nu\rangle}{E + i\delta + E_\nu - E_\mu}\left[exp(-\beta E_\mu) + exp(-\beta E_\nu)\right],$$

where $\mu, \nu < \xi$ means $E_\mu, E_\nu < E_\xi$. Than the condition can be written as

$$\xi > \zeta \quad \not\Rightarrow \quad |G^\xi(E) - G(E)| > |G^\zeta(E) - G(E)|$$

To understand when could this condition be fulfilled one should imagine the case $|E + E_\nu - E_\mu| \ll 1$, i.e. the energy point E where Green's function is evaluated negligible differs from the $|E_\nu - E_\mu|$. Of cause, one can say that it does not matter because due to $exp[-\beta E_\nu]$ factor. Namely, the summation has to be evaluated up to ν fulfilled $exp[-\beta E_\nu] \ll 1$. Well, it is true. But it

will be nice to have a certain criteria to make cutoff of summation in (4.6). Now, comes the good news: the Lanczos method does not suffer from these problems. It allows to solve partial eigenproblem and supplies with iterative convergence algorithm for evaluating Green's function (4.6). Since the case of finite temperature has no principle differences from the zero temperature case the latter will be considered in detail. Then the finite temperature extension will be specified.

4.1 The Lanczos method

The Lanczos method is based on iterative algorithm. The initial vector to start iterations $|\nu_0\rangle$ is chosen. The considerations of the choice will be discussed later. Then using Hamiltonian $\hat{H}$ as generator, new vectors are produced. The set of vectors is called the Lanczos basis. The iterative procedure to construct Lanczos correspond to:

$$
\begin{aligned}
|\nu_1\rangle &= \hat{H}|\nu_0\rangle - \frac{\langle\nu_0|\hat{H}|\nu_0\rangle}{\langle\nu_0|\nu_0\rangle}|\nu_0\rangle, \\
|\nu_2\rangle &= \hat{H}|\nu_1\rangle - \frac{\langle\nu_1|\hat{H}|\nu_1\rangle}{\langle\nu_1|\nu_1\rangle}|\nu_1\rangle - \frac{\langle\nu_1|\nu_1\rangle}{\langle\nu_0|\nu_0\rangle}|\nu_0\rangle, \\
|\nu_3\rangle &= \hat{H}|\nu_2\rangle - \frac{\langle\nu_2|\hat{H}|\nu_2\rangle}{\langle\nu_2|\nu_2\rangle}|\nu_2\rangle - \frac{\langle\nu_2|\nu_2\rangle}{\langle\nu_1|\nu_1\rangle}|\nu_1\rangle
\end{aligned}
$$

It can be easily checked that $\langle\nu_0|\nu_1\rangle = 0$, $\langle\nu_1|\nu_2\rangle = 0$ and so on. In general, the iterative procedure is specified as follows:

$$
|\nu_{i+1}\rangle = \hat{H}|\nu_i\rangle - a_i|\nu_i\rangle - b_i^2|\nu_{i-1}\rangle, \tag{4.8}
$$

$$
\text{where} \quad a_i = \frac{\langle\nu_i|\hat{H}|\nu_i\rangle}{\langle\nu_i|\nu_i\rangle},
$$

$$
b_i^2 = \frac{\langle\nu_i|\nu_i\rangle}{\langle\nu_{i-1}|\nu_{i-1}\rangle}
$$

with $b_0^2 \equiv 0$ and $|\nu_{-1}\rangle \equiv 0$.

Now, the application this algorithm for partial eigenvalue problem is under consideration. The initial state $|\nu_0\rangle$ should have nonzero overlap with the ground state [31, 32]. If no *a priori* information about ground state is known than arbitrary initial vector $|\nu_0\rangle$ is chosen. But if it is known that the ground state belongs to the invariant part of Hilbert space described by some

quantum numbers then the initial vector should belong to the same part of Hilbert space.

The basis construction proceeds until the Hilbert space dimension is reached (when full eigenproblem is demanded to be solved) or convergence criterion is fulfilled. The latter could be $\langle \nu_{i+1} | \nu_{i+1} \rangle < \varepsilon$. This procedure brings the Hamiltonian to the tridiagonal form:

$$H = \begin{bmatrix} a_0 & b_1 & 0 & 0 & \cdots \\ b_1 & a_1 & b_2 & 0 & \cdots \\ 0 & b_2 & a_2 & b_3 & \cdots \\ 0 & 0 & b_3 & a_3 & \cdots \\ \vdots & \vdots & \vdots & \vdots & \ddots \end{bmatrix} \tag{4.9}$$

In principle, this tridiagonal sparse matrix could be easy diagonalized by standard mathematic subroutines [33, 34, 35] and full eigenproblem (when the Lanczos basis covers the whole Hilbert space) could be solved. In practice it is not so, because of a problem with stability. Stability means how much the algorithm will be affected (i.e. will it produce the approximate result close to the original one) if there are small numerical errors introduced and accumulated.

For the Lanczos algorithm, it can be proved that with exact arithmetic, the set of vectors $|\nu_0\rangle, |\nu_1\rangle, \ldots, |\nu_m\rangle$ constructs an orthogonal basis, and the eigenvalues/eigenvectors solved are good approximation to those of original matrix. However, in practice (as the calculations are performed in floating point arithmetic where inaccuracy is inevitable), the orthogonality is quickly lost and in some cases the new vector could even be linearly dependent on the set that is already constructed. As the result, some of the eigenvalues of the resultant tridiagonal matrix may not be approximations to the original matrix. Therefore, the Lanczos algorithm is not very stable.

Nevertheless the ground state could be precisely obtained and correspond dynamical properties could be easily found by the Lanczos scheme.The great advantage of algorithms is a fast convergence. About 100 iterations or less is sufficient to reach ground state with a great accuracy. Common explanation for this rapid convergence lays in nature of iterative diagonalization methods. They are based on an idea to project the matrix to be treated H onto a subspace of dimension $M \ll N$ (where N is the dimension of the Hilbert space in which the diagonalization is carried out). The latter is cleverly chosen so that the extremal eigenstates within the subspace converge very quickly with M to the extremal eigenstates of the system.

It could be illustrated explicitly on two examples. The first is very simple power method. In this approach, the eigenvector with the extremal eigen-

value is obtained by repeatedly applying the Hamiltonian to a random initial state $|\nu_0\rangle$,

$$|\nu_n\rangle = \hat{H}^n|\nu_0\rangle$$

Expanding in the eigenbasis $\hat{H}|i\rangle = E_i|i\rangle$ yields

$$\begin{aligned} |\nu_n\rangle &= \sum_i \langle i|\nu_0\rangle \, \hat{H}^n|i\rangle \\ &= \sum_i \langle i|\nu_0\rangle \, E_i^n|i\rangle \end{aligned}$$

It is clear that the state with eigenvalue with the largest absolute value will have highest weight after many iterations n, provided that $|\nu_0\rangle$ has a finite overlap with this state. The subspace generated by the sequence of steps on the power method

$$\{|\nu_0\rangle, \hat{H}|\nu_0\rangle, \hat{H}^2|\nu_0\rangle, ..., \hat{H}^n|\nu_0\rangle\}, \tag{4.10}$$

is called the n^{th} Krylov space and is the starting point for the other procedures.

The convergence behavior is determined by the spacing between the extremal eigenvalue and the next one. In any case, with every new step a better approximation for the ground state is obtained. All these is true for the Lanczos method as due to the orthogonal basis produced and therefore more fast convergence is supplied.

The second algorithm is known as modified Lanczos method [36, 37]. The iterative procedure consist of "2x2" steps. Namely, $|\nu_0\rangle$, $|\nu_1\rangle$ basis is constructed and the $\hat{H}$ represented in this basis is diagonalized. The lower energy state is taken as the initial for the generation new pair of basis set $|\nu_0'\rangle$, $|\nu_1'\rangle$ and so on. And again new variational state represented the ground state is improved in systematic way.

In spite of the advantage of this method the memory limitation impose the significant restriction on the size of the cluster to be treated. To understand this point note that the ground state is written as $|\psi_0\rangle = \sum_i |f_i\rangle$, where each $|f_i\rangle$ basis vector should be expressed in some convenient basis which Hamiltonian be easy applied to. For instance,in Hubbard model the state of each site is specified four state basis : $|0\rangle$, $|\uparrow\rangle$, $|\downarrow\rangle$, $|2\rangle$. The basis dimension grows exponentially. In result, for $N_{site} = 16$ the total dimension of Hilbert space is $4^{16} \approx 4.3 \times 10^9$. Such a memory requirement is unreachable for now-days computers. Fortunately, this problem can be reduced using the symmetry of the problem to represent the Hamiltonian in a block-diagonal form. The most obvious symmetry is the number of particles which is usually

conserved. The total projection of spin S^z_{total} might also be a good quantum number. For example, if both number of particle $N_{particle}$ and total spin S^z_{total} are conserved than the linear size of the Hamiltonian block to be diagonalized is 12870. The importance of symmetry using is evidence.

How we can obtain the ground state exactly? Each element of Lanczos basis $|\nu_i\rangle$ is represented by a set of coefficients which number is the size of work basis. In the same time the ground state is expressed by a coefficient set $|\psi_0\rangle = \sum_i c_i|\nu_i\rangle$. Taking into account the number of iterations are required to reach the ground state (~ 100) it has to conclude that storing the whole Lanczos basis is not convenient. The decision is very simple - run Lanczos procedure twice. First - to obtain coefficients of ground state representation in Lanczos basis . Second - to restore Lanczos basis vectors (for Lanczos itself only three vectors is demanded to be store in memory).

4.2 Dynamical properties

4.2.1 Zero temperature

The ability to calculate dynamic properties with fine convergence and in stable way is the one of the most appealing feature of the Lanczos technique. Stability is due to the recursion method, i.e. it is the property of clever numeric scheme. For convenience we derive the required expression of the Green's function at zero temperature. The finite temperature extension will be derived later.

We start from (4.6):

$$G_{ij}(i\omega_n) = \frac{1}{Z}\sum_{\mu,\nu}\frac{\langle\nu|c_i|\mu\rangle\langle\mu|c_j^+|\nu\rangle}{i\omega_n + E_\nu - E_\mu}\left[exp(-\beta E_\mu) + exp(-\beta E_\nu)\right]$$

Let us regroup the terms

$$G_{ij}(i\omega_n) = \frac{1}{Z}\sum_{\mu,\nu}\frac{\langle\mu|c_j^+|\nu\rangle\langle\nu|c_i|\mu\rangle}{i\omega_n + E_\nu - E_\mu}exp(-\beta E_\mu) + \frac{1}{Z}\sum_{\mu,\nu}\frac{\langle\nu|c_i|\mu\rangle\langle\mu|c_j^+|\nu\rangle}{i\omega_n + E_\nu - E_\mu}exp(-\beta E_\nu)$$

Now, one performs the limit of $\beta \to \infty$ after shift $E \to E - E_0$ (E_0 - is a ground state energy) and change $\nu \to \mu$ in the first term

$$G_{ij}(i\omega_n) = \sum_\mu\left\{\frac{\langle 0|c_j^+|\mu\rangle\langle\mu|c_i|0\rangle}{i\omega_n + E_\mu} + \frac{\langle 0|c_i|\mu\rangle\langle\mu|c_j^+|0\rangle}{i\omega_n - E_\mu}\right\} \tag{4.11}$$

For recursion method it is required to rewrite last expression to contain Hamiltonian $\hat{H}$ instead of eigenenergies E_μ. We make this trick with the first term:

$$\sum_\mu \frac{\langle 0|c_j^+|\mu\rangle\langle\mu|c_i|0\rangle}{iw_n + E_\mu} =$$
$$\sum_\mu \langle 0|c_j^+(\hat{H} + iw_n)^{-1}|\mu\rangle\langle\mu|c_i|0\rangle =$$
$$\langle 0|c_j^+(\hat{H} + iw_n)^{-1}\sum_\mu |\mu\rangle\langle\mu|c_i|0\rangle =$$
$$\langle 0|c_j^+\frac{1}{iw_n + \hat{H}}c_i|0\rangle$$

The second term can be written in the similar way

$$\sum_\mu \frac{\langle 0|c_i|\mu\rangle\langle\mu|c_j^+|0\rangle}{i\omega_n - E_\mu} =$$
$$\langle 0|c_i\frac{1}{iw_n - \hat{H}}c_j^+|0\rangle$$

As the result

$$G_{ij}(iw_n) = \langle 0|c_i\frac{1}{iw_n - \hat{H}}c_j^+|0\rangle + \langle 0|c_j^+\frac{1}{iw_n + \hat{H}}c_i|0\rangle \qquad (4.12)$$

This is exactly the form which Lanczos (recursion) method deals with. For the simplicity we consider the diagonal case

$$\begin{aligned} G_{ii}(iw_n) &= \langle 0|c_i\frac{1}{iw_n - \hat{H}}c_i^+|0\rangle + \langle 0|c_i^+\frac{1}{iw_n + \hat{H}}c_i|0\rangle \equiv \\ G(iw_n) &= \langle 0|c\frac{1}{iw_n - \hat{H}}c^+|0\rangle + \langle 0|c^+\frac{1}{iw_n + \hat{H}}c|0\rangle \end{aligned} \qquad (4.13)$$

Only the first term is considered. To evaluate this expression the Hamiltonian will be brought to tridiagonal form by the standard Lanczos recursion relations. But instead of starting from a random vector as in evaluating the ground state $|0\rangle$ we choose the initial vector as

$$|\phi_0\rangle = \frac{c^+|0\rangle}{\sqrt{\langle 0|c\,c^+|0\rangle}} \qquad (4.14)$$

and build Lanczos basis

$$|\phi_{k+1}\rangle = \hat{H}|\phi_k\rangle - a_k|\phi_k\rangle - b_k^2|\phi_{k-1}\rangle, \tag{4.15}$$

$$\text{where} \quad a_k = \frac{\langle\phi_k|\hat{H}|\phi_k\rangle}{\langle\phi_k|\phi_k\rangle},$$

$$b_k^2 = \frac{\langle\phi_k|\phi_k\rangle}{\langle\phi_{k-1}|\phi_{k-1}\rangle}$$

with $b_0^2 \equiv 0$ and $|\phi_{-1}\rangle \equiv 0$. To understand this choice let us consider the identity:

$$(z - \hat{H})(z - \hat{H})^{-1} \;=\; I,$$

or in details:

$$\sum_n (z - \hat{H})_{mn}(z - \hat{H})^{-1}_{np} \;=\; \delta_{mp}, \tag{4.16}$$

where $\hat{H}$ is a Hamiltonian (represented in Lanczos basis $|\phi_n\rangle$ with $|\phi_0\rangle$ defined in (4.14)) and z - complex variable. With $p = 0$ (4.16) becomes system of linear equations :

$$\sum_n (z - \hat{H})_{mn} x_n \;=\; \delta_{m0} \tag{4.17}$$

Where $\left[\vec{x}\right]_n = (z - \hat{H})^{-1}_{n0}$ is vector to be calculated. The first component of $\vec{x}$ is

$$x_0 = (z - \hat{H})^{-1}_{00} = \langle\phi_0|\frac{1}{z - \hat{H}}|\phi_0\rangle, \tag{4.18}$$

exactly what we are interested in (see (4.12)). Cramer's rules is used to evaluate x_0

$$x_0 = \frac{\|\hat{B}_0\|}{\|z - \hat{H}\|}, \tag{4.19}$$

where

$$z - \hat{H} = \begin{bmatrix} z - a_0 & -b_1 & 0 & 0 & \dots \\ -b_1 & z - a_1 & -b_2 & 0 & \dots \\ 0 & -b_2 & z - a_3 & -b_3 & \dots \\ \vdots & \vdots & \vdots & \vdots & \end{bmatrix}, \tag{4.20}$$

and

$$B_0 = \begin{bmatrix} 1 & -b_1 & 0 & 0 & \dots \\ 0 & z-a_1 & -b_2 & 0 & \dots \\ 0 & -b_2 & z-a_3 & -b_3 & \dots \\ \vdots & \vdots & \vdots & \vdots & \end{bmatrix}, \tag{4.21}$$

with the coefficients a_n, b_n defined in Lanczos (4.15). Introducing denotations D_i as matrices with excluded $1 \dots i$ -rows and columns from $\left[z - \hat{H}\right]$ we get

$$\|z - \hat{H}\| = (z - a_0)\|D_1\| - b_1^2\|D_2\|,$$

$$\|B_0\| = \|D_1\|$$

Therefore x_0 can be found

$$x_0 = \frac{1}{z - a_0 - b_1^2 \dfrac{\|D_2\|}{\|D_1\|}} \tag{4.22}$$

The ratio of determinants in denominator in (4.22) is easy evaluated in similar manner

$$\frac{\|D_2\|}{\|D_1\|} = \frac{1}{z - a_1 - b_2^2 \dfrac{\|D_3\|}{\|D_2\|}} \tag{4.23}$$

This procedure is repeated until the continued fraction is constructed

$$\langle\phi_0|\frac{1}{z-\hat{H}}|\phi_0\rangle = \cfrac{1}{z - a_0^> - \cfrac{{b_1^>}^2}{z - a_1^> - \cfrac{{b_2^>}^2}{z - a_2^> \cdots}}} \tag{4.24}$$

where the coefficients $a_i^>$ and ${b_i^>}^2$ with ">" upper subscript are obtained in Lanczos procedure with $c^+|0\rangle$ as the initial vector. In the same manner the corresponding expression for the second term in (4.12) is found

$$\langle\phi_0|\frac{1}{z+\hat{H}}|\phi_0\rangle = \cfrac{1}{z + a_0^< - \cfrac{{b_1^<}^2}{z + a_1^< - \cfrac{{b_2^<}^2}{z + a_2^< \cdots}}} \tag{4.25}$$

where again the coefficients $a_i^<$ and $b_i^{<2}$ with "$<$" upper subscript are obtained in Lanczos procedure with $c|0\rangle$ initial vector.
Finally, we obtained:

$$G(iw_n) = G^>(iw_n) + G^<(iw_n) = \tag{4.26}$$
$$\frac{\langle 0|c\, c^+|0\rangle}{iw_n - a_0^> - \dfrac{b_1^{>2}}{iw_n - a_1^> - \dfrac{b_2^{>2}}{iw_n - a_2^< \cdots}}} + \frac{\langle 0|c^+ c|0\rangle}{iw_n + a_0^> - \dfrac{b_1^{>2}}{iw_n + a_1^> - \dfrac{b_2^{>2}}{iw_n + a_2^> \cdots}}}$$

4.2.2 Finite Temperature

The starting point to modify Lanczos technique for a finite temperature again is the Green's function in Lehmann representation (4.6)

$$G_{ij}(i\omega_n) = \frac{1}{Z}\sum_{\mu,\nu} \frac{\langle\nu|c_i|\mu\rangle\langle\mu|c_j^+|\nu\rangle}{i\omega_n + E_\nu - E_\mu}\left[exp(-\beta E_\mu) + exp(-\beta E_\nu)\right]$$

This formula could be easy rewritten in different manner:

$$G_{ij}(i\omega_n) = \frac{1}{Z}\sum_\nu e^{-\beta E_\nu}\left\{\sum_\mu \frac{\langle\nu|c_i|\mu\rangle\langle\mu|c_j^+|\nu\rangle}{i\omega_n + E_\nu - E_\mu} + \frac{\langle\nu|c_j^+|\mu\rangle\langle\mu|c_i|\nu\rangle}{i\omega_n + E_\mu - E_\nu}\right\} \tag{4.27}$$

The expression inside the curly braces is equivalent to (4.11) only with substitution $|0\rangle$ for $|\nu\rangle$. So we can see that only low-energy eigenstates due to a factor $e^{-\beta\nu}$ factor are required. To obtain precisely these states we used the Arnoldi algorithm [38]. It is like Lanczos algorithms only with the stabilizes Gram-Schmidt process , i.e. at each iteration new vector is orthogonalized to previous ones. Latter decides the stability problem consisted in orthogonality loss. Summarizing all written above, came to the following expression:

$$G(iw_n) = \frac{1}{Z}\sum_\nu e^{-\beta E_\nu}[G^>(iw_n) + G^<(iw_n)], \tag{4.28}$$

where $G^>(iw_n)$ and $G^<(iw_n)$ are evaluated as

$$G^{\nu>}(iw_n) = \frac{\langle\nu|c\, c^+|\nu\rangle}{iw_n - a_0^> - \dfrac{b_1^{>2}}{iw_n - a_1^> - \dfrac{b_2^{>2}}{iw_n - a_2^> \cdots}}} \tag{4.29}$$

$$G^{\nu<}(iw_n) = \cfrac{\langle\nu|c^+c|\nu\rangle}{iw_n + a_0^< - \cfrac{b_1^{<2}}{iw_n + a_1^< - \cfrac{b_2^{<2}}{iw_n + a_2^< \cdots}}} \tag{4.30}$$

In practice the sum over eigenstates in(4.28) is restricted due to the $e^{-\beta E_\nu}$ factor. Therefore analog of (4.28) for real calculations looks

$$G(iw_n) = \frac{1}{Z}\sum_{\nu=1}^{N_{arnoldi}} e^{-\beta E_\nu}[G^>(iw_n) + G^<(iw_n)], \tag{4.31}$$

where $N_{arnoldi}$ is the number of first low-energy eigenstates taken into account.

4.3 Test calculations

Now after all preliminaries were made we can check the efficient of the Temperature Lanczos (Arnoldi) algorithm to compare it with the full diagonalization. One this comparison is made for the Anderson impurity model shown on fig. 4.1.

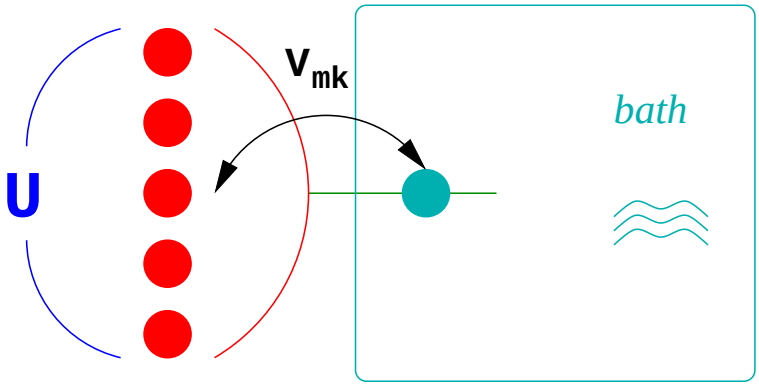

Figure 4.1: Anderson impurity model with $N_s = 6 \quad N_{imp} = 5 \quad N_{bath} = 1$

From this picture it is clear that N_s denotes the total number of sites in Anderson impurity model (AIM). Then correspondingly N_{imp} - the number of impurity orbitals, N_{bath} - the number of sites in the bath ($N_s = N_{imp} + N_{bath}$). It is convenience to take some notations. Let's call the Anderson impurity model with N_{imp} and N_{bath} as $N_{imp} + N_{bath}$. For instance, the AIM with 5 impurity orbitals and 1 orbital in bath is called $5 + 1$ AIM.

The hybridization parameters are assumed symmetric and equal $\forall\, m\; V_{m1} = 0.2\; eV$ ($k = 1$ - only one bath orbital). The energy of the bath orbital $\varepsilon_1 = -0.6\; eV$. Full $\hat{U}$ matrix is calculated with parameters $U = 4\,eV$ $J = 0.5\,eV$, where as usual

$$U = \frac{1}{(2l+1)^2}\sum_{i,j} U_{ijji} \tag{4.32}$$

$$J = U - \frac{1}{2l(2l+1)}\sum_{i,j} U_{ijij}. \tag{4.33}$$

First we check the case of temperature where Lanczos ($N_{arnoldi} = 1$) should work well. The inverse temperature is fixed $\beta = 2 \cdot 10^4\; eV (T < 1$ K). Only chemical potential μ ($\varepsilon_d = -\mu$) is varying. On all figures label ED means full diagonalization. At Figure 4.2 we can see that calculation with $N_{arnoldi} = 1$

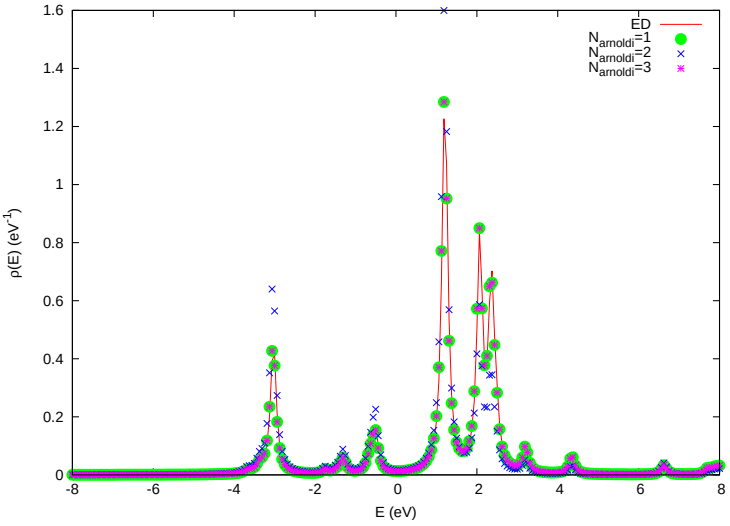

Figure 4.2: Density of States for $5+1$ Anderson impurity model at $\beta = 2 \cdot 10^4\, eV^{-1}$, $\mu = 6$ eV, $U = 4\,eV$, $J = 0.5\,eV$, $\varepsilon_{imp} = -\mu$, $\varepsilon_{bath} = -0.6\,eV$, $V_{km} = 0.2\,eV$

reproduces the density of states obtained with full diagonalization. It is again true for $N_{arnoldi} = 3$ what is obviously at this temperature. But in the case of $N_{arnoldi} = 2$ we see disagreement. It can be understood by analyzing the multiplet structure of the spectrum. At $\mu = 6\,eV$ the degree of degeneracy of the system's ground state is three. They belong to follow sectors $(n_\uparrow, n_\downarrow)$:

$(3,1)$, $(1,3)$ and $(2,2)$. If we take $N_{arnoldi} = 1$ than we obtain the ground state from $(2,2)$ sector. In the case of $N_{arnoldi} = 2$ we obtain the ground states from $(2,2)$ and $(1,3)$ sectors. Let us to introduce some notations:

$$N_{g.s} - \text{total number of ground states } |\nu\rangle$$

$$\begin{aligned} a \equiv &\{|ground\,state\rangle \in (1,3)\} \\ b \equiv &\{|ground\,state\rangle \in (3,1)\} \\ c \equiv &\{|ground\,state\rangle \in (2,2)\} \end{aligned}$$

$$G^{true}(i\omega_n) = \sum_{\nu=1}^{N_{g.s.}} \sum_{\mu} \left\{ \frac{\langle\nu|c^+|\mu\rangle\langle\mu|c|\nu\rangle}{i\omega_n + E_\mu} + \frac{\langle\nu|c|\mu\rangle\langle\mu|c^+|\nu\rangle}{i\omega_n - E_\mu} \right\}$$

$$G^{full}(i\omega_n) = \sum_{\nu=1}^{N_{arnoldi}} \sum_{\mu} \left\{ \frac{\langle\nu|c^+|\mu\rangle\langle\mu|c|\nu\rangle}{i\omega_n + E_\mu} + \frac{\langle\nu|c|\mu\rangle\langle\mu|c^+|\nu\rangle}{i\omega_n - E_\mu} \right\}$$

$$G^{\zeta}(i\omega_n) = \sum_{\nu=\zeta} \sum_{\mu} \left\{ \frac{\langle\nu|c^+|\mu\rangle\langle\mu|c|\nu\rangle}{i\omega_n + E_\mu} + \frac{\langle\nu|c|\mu\rangle\langle\mu|c^+|\nu\rangle}{i\omega_n - E_\mu} \right\},$$

where

$$\zeta = a, b \text{ or } c$$

and the orbital indexes are omitted because of the symmetry

$$G_{ii} = G_{jj}\ \forall\, i,j$$

From the Fig. 4.2 we can establish that:

$$\begin{aligned} G^{true} =& G^c \\ G^{true} =& \frac{1}{3}(G^a + G^b + G^c) \end{aligned}$$

Than for $N_{arnoldi} = 2$ we derive:

$$G^{full} = \frac{1}{2}(G^a + G^c) = \frac{1}{2}(G^a + G^{true}) \neq G^{true}$$

So, the disagreement for $N_{arnoldi} = 2$ is explained by the symmetry of ground states. We conclude that the ground state from $(2,2)$ sector has the symmetry of the system in sense: $G^{true} = G^c$.

Another interesting case is $\mu = 9\,eV$ represented at Fig. 4.3. Here the calculation with $N_{arnoldi} = 1$ does not fit the full diagonalization density of states. While $N_{arnoldi} = 4$ does. The explanation is again contained in the structure of the spectrum. The ground state is four times degenerate. The

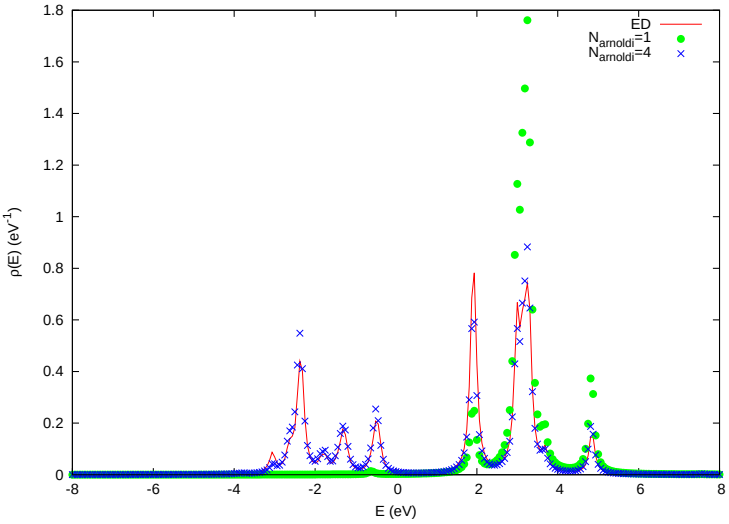

Figure 4.3: Density of States for $5+1$ Anderson impurity model at $\beta = 2 \cdot 10^4\, eV^{-1}$, $\mu = 9\, eV$, $U = 4\, eV$, $J = 0.5\, eV$, $\varepsilon_{imp} = -\mu$, $\varepsilon_{bath} = -0.6\, eV$, $V_{km} = 0.2\, eV$

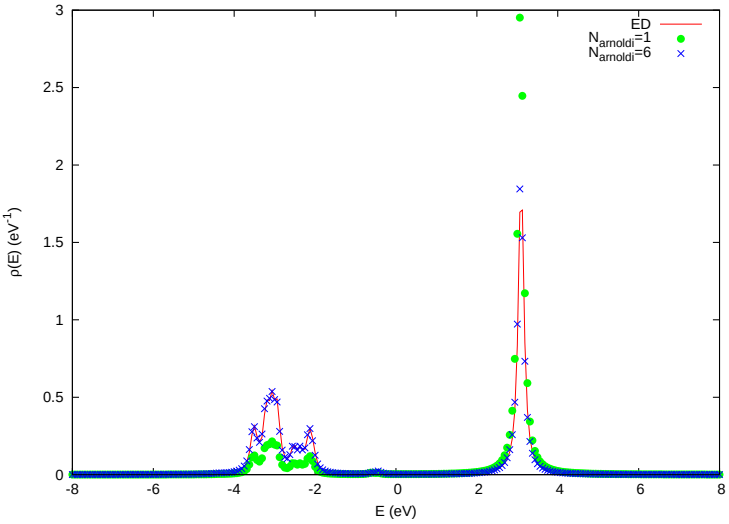

Figure 4.4: Density of States for $5+1$ Anderson impurity model at $\beta = 2 \cdot 10^4\, eV^{-1}$, $\mu = 17\, eV$, $U = 4\, eV$, $J = 0.5\, eV$, $\varepsilon_{imp} = -\mu$, $\varepsilon_{bath} = -0.6\, eV$, $V_{km} = 0.2\, eV$

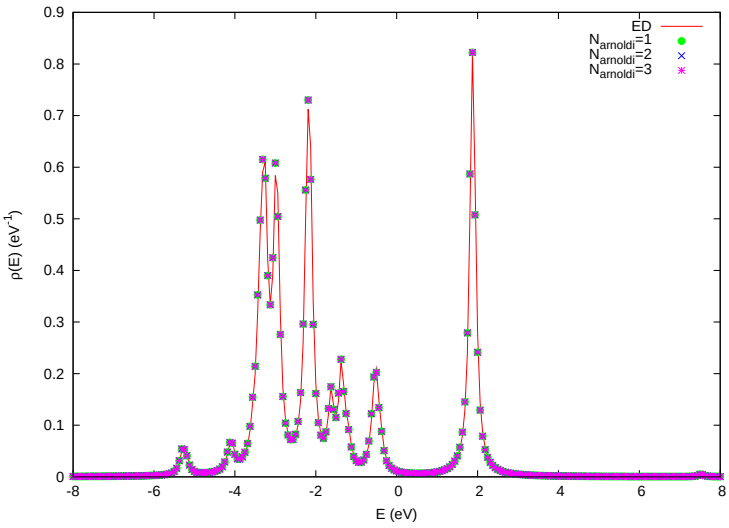

Figure 4.5: Density of States for $5+1$ Anderson impurity model at $\beta = 2 \cdot 10^4\, eV^{-1}$, $\mu = 29\, eV$, $U = 4\, eV$, $J = 0.5\, eV$, $\varepsilon_{imp} = -\mu$, $\varepsilon_{bath} = -0.6\, eV$, $V_{km} = 0.2\, eV$

sectors $(n_\uparrow, n_\downarrow)$ where they lie are follows: $(3,2)$, $(2,3)$, $(4,1)$ and $(1,4)$. It is evidence that no one can choose only one ground state without braking the symmetry. The consideration of all ground states obviously gives correct DOS. The scalculation with $N_{arnoldi} = 6$ is shown at the same Fig. 4.3 to demonstrate that at the temperature $\beta = 2 \cdot 10^4\, eV^{-1}$ only ground states are important for this system because other states have to high energy.

The value $\mu = 17\, eV$ correspond to half-filling case. It is expected the ground state to be most degenerate. It is true - the ground state is six times degenerate. And again $N_{arnoldi} = 1$ cannot reproduce true density of states because of even number of ground states. Only calculation $N_{arnoldi} = 6$ reproduces DOS obtained with exact diagonalization.

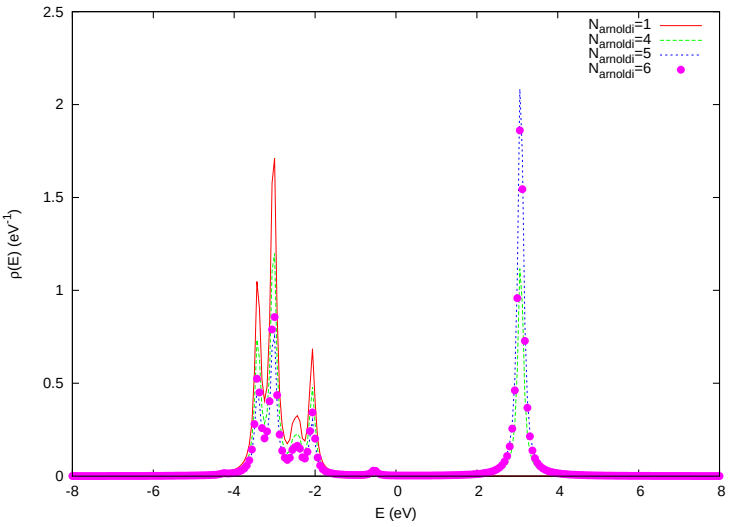

Figure 4.6: Density of States for $5+5$ Anderson impurity model at $\beta = 2 \cdot 10^4\, eV^{-1}$, $\mu = 26\, eV$, $U = 4\, eV$, $J = 0.7\, eV$, $\varepsilon_{imp} = -\mu$, $\varepsilon_{bath} = -0.6\, eV$, $V_{km} = 0.2\, eV$

Now, let us consider the case of $\mu = 29\, eV$. It is shown on Fig. 4.5. It is a very interesting case. The ground state is three times degenerate and the sectors contained these states are $(5,5)$, $(6,4)$ and $(4,6)$. How it could be that calculations with $N_{arnoldi} = 1, 2$ and 3 all fit the correct DOS? The case $N_{arnoldi} = 3$ does not require the explanations. The answer for $N_{arnoldi} = 1, 2$ is an agreement with conclusions described above. The chosen set of ground states does not brake the symmetry. Namely, at $N_{arnoldi} = 1$ we get the ground state from $(5,5)$ sector while at $N_{arnoldi} = 2$ we obtain two ground states form $(6,4)$ and $(4,6)$ sectors. This situation is very similar to the

case $\mu = 6\,eV$. The only diference chosing two ground states we remain the symmetry of the system.

Let us now consider the $5+5$ Anderson impurity model. First calculation is made for the temperature $\beta = 2 \cdot 10^4\,eV^{-1}$ at $\mu = 17\,eV$ corresponding to half-filling (Fig. 4.6). The ground state is six times degenerate. One can see that DOS calculated with $N_{arnoldi} = 1$ does not contain electron pick at $-3\,eV$. Ground states lie in $(n_\uparrow, n_\downarrow)$ sectors: $(5, 10)$,$(10, 5)$,$(6, 9)$,$(9, 6)$,$(7, 8)$ and $(8, 7)$. The calculations with $N_{arnoldi} = 4$ and $N_{arnoldi} = 4$ contain ground states from sectors: $(7, 8)$, $(8, 7)$, $(9, 6)$, $(10, 5)$ and $(7, 8)$, $(8, 7)$, $(9, 6)$, $(10, 5)$, $(5, 10)$ correspondingly. One can see that DOS obtained in calculation with $N_{arnoldi} = 4$ significally differs from $N_{arnoldi} = 6$ (which considered all ground states) while other one with $N_{arnoldi} = 5$ fit $N_{arnoldi} = 6$ very well. It looks like ground state from $(9, 6)$ (or $(6, 9)$) sector has the symmetry of the whole system. It should be explained in more details. When we speak about the symmetry of a gound state we actually mean that Green's function built on this ground state (4.29) and (4.30) describes the same transitions to excited states with the same amplitudes as the full Green's function (4.31).

The other calculation for $5 + 5$ AIM carried out with parameters $\beta = 40\,eV^{-1}$ and $\mu = 26\,eV$ is represented on Fig. 4.7. The ground state is four times degenerate. We can see that it is not sufficient to take into account all ground states at this temperature. One extra excited state were found (four times degenerated). We can see that with the increasing of temperature DOS has more picks and they become broader. It is because the excited states become important.

The tests discussed above show that one has to take into account a multiplet structure of the spectrum to explain the results. This structure could have a complicated symmetry. We showed that the finite temperature Lanczos method is important not only at finite temperatures but also at zero temperature in the case of degenerate ground state.

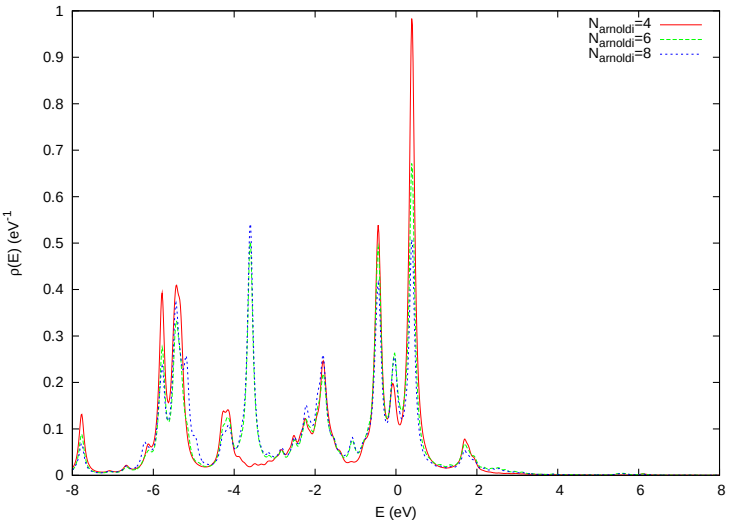

Figure 4.7: Density of States for $5+5$ Anderson impurity model at $\beta = 40\,eV^{-1}$, $\mu = 26\,eV$, $U = 4\,eV$, $J = 0.7\,eV$, $\varepsilon_{imp} = -\mu$, $\varepsilon_{bath}^{t_{2g}} = -0.2\,eV$, $\varepsilon_{bath}^{t_{eg}} = 0.3\,eV$, $V_{km} = 0.4\,eV$

Chapter 5

Double Counting in LDA+DMFT – The Example of NiO

5.1 Introduction

The combination of the density functional theory (DFT/LDA), a model Hamiltonian and the dynamical mean field approximation (DMFT) [23], a methodology commonly referred to as LDA+DMFT, is to date one of the best approaches for the realistic description of strongly correlated electron systems [39, 40]. While density functional theory does not include all the interactions between strongly correlated d or f electrons, it captures some portion of them through the Hartree and exchange-correlation terms. By introduction of a model Hamiltonian into the calculations one tries to account for as much of the interactions as possible through the Coulomb interaction matrix of the impurity model. This ultimately leads to the problem that some contributions to the interaction are included twice. This has to be explicitly compensated by adding a shift in the chemical potential of the correlated orbitals to the Hamiltonian, leading to the prominent issue of double counting. The LDA+DMFT Hamiltonian can be written as follows

$$\begin{aligned} H = \quad & H_{LDA} - H_{dc} + \\ & + \tfrac{1}{2} \sum_{i,\sigma\sigma',mm'm''m'''} U_{mm'm''m'''} c^{\dagger}_{im\sigma} c^{\dagger}_{im'\sigma'} c_{im'''\sigma} c_{im''\sigma} \end{aligned}$$

where H_{LDA} is the LDA Hamiltonian, $c^{\dagger}_{im\sigma}$ creates a particle with spin σ in a localized orbital m at site i and $U_{mm'm''m'''}$ is the Coulomb interaction matrix

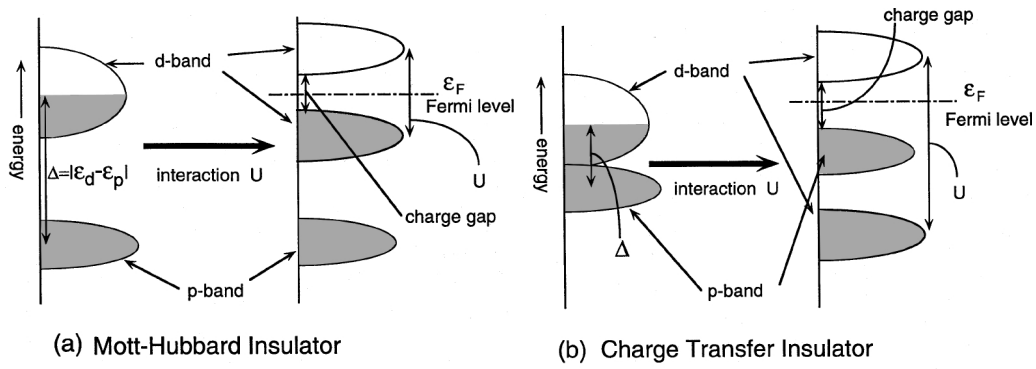

Figure 5.1: Schematic illustration of the effect of the Coulomb interaction on the energy levels in a Mott-Hubbard (a) and a charge transfer insulator (b). Figure from [45].

between localized orbitals. Above Hamiltonian contains the double-counting correction

$$H_{dc} = \mu_{dc} \sum_{m,\sigma} n_{m,\sigma},$$

where $n_{m,\sigma} = c^\dagger_{m\sigma} c_{m\sigma}$ and μ_{dc} is the double-counting potential. How to choose the double-counting potential in a manner that is physically sound and consistent is unknown and systematic investigations of the effects of the double counting in LDA+DMFT on the spectrum are seldom performed. In the work presented here we attempt to shed some light on the double-counting problem using the example of nickel oxide (NiO). In recent years a number of authors applied the LDA+DMFT method in different flavors to this system generating a body of promising results [41, 42, 43, 44].

5.2 NiO – a charge transfer system

Nickel oxide is a strongly correlated transition metal oxide that is a prototypic member of the class of charge transfer insulators. According to Zaanen, Sawatzky and Allen transition metal oxides can exhibit a behavior different to the classic Mott-Hubbard picture [46]. In a Mott-Hubbard insulator the charge gap opens through splitting of the d band by the Hubbard U. In the charge-transfer system the gap typically opens between hybridized ligand p and transition metal d states and the upper Hubbard band corresponding to the d states of the transition metal. Thus, it is not only the Hubbard U, but also the so called charge transfer energy $\Delta = |\varepsilon_d - \varepsilon_p|$ that determines the size of the gap. In the scheme by Zaanen, Sawatzky and Allen materials can be classified by their respective values of U and Δ [47]. For $\Delta > U$ the

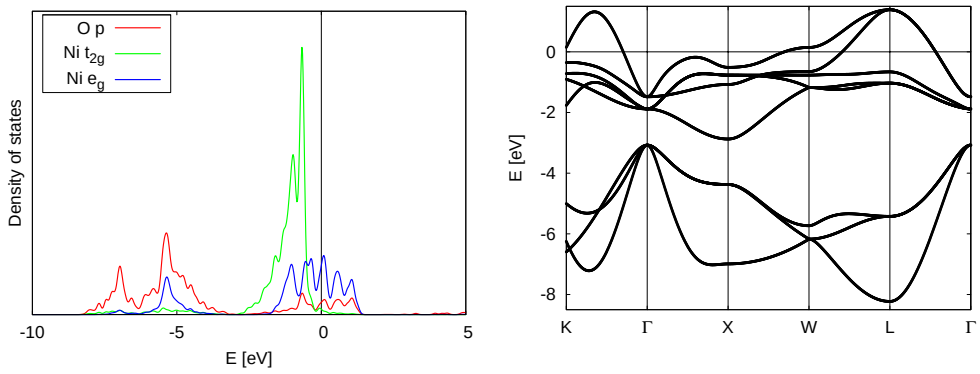

Figure 5.2: Density of states (left) and band structure (right) of NiO as obtained by LDA calculations. In the band structure the 5 bands crossing the Fermi level are Ni $3d$ bands, the 3 bands below correspond to oxygen $2p$ states. For further details we refer to the text.

system is a Mott-Hubbard insulator, whereas for $\Delta < U$ it belongs to the charge transfer class. In general, systems with completely filled $d(e_g)$ and partially filled $d(t_{2g})$ shells, like titanates, vanadates and some ruthenates belong to the Mott-Hubbard class. Prominent examples of charge transfer insulators are NiO, MnO, manganites and cuprates. In these systems the e_g shell is partially filled and the t_{2g} shell is fully occupied.

The density of states and the band structure of NiO as obtained by LDA (using the PAW [48] based VASP code [49]) are shown in Fig.(5.2). The band structure shows five Ni $3d$ bands in the energy window -2.5eV to $+1.5$eV crossing the Fermi energy and three separated O $2p$ bands below, extending down to -8eV. These bands contain 14 electrons in total, 6 occupy the oxygen p bands and the remaining 8 the Ni d bands. In contrast to the LDA prediction NiO is not a metal, on the contrary, experiments revealed a charge gap of about 4eV [50]. Additionally, it exhibits antiferromagnetic order below the Néel temperature of $T_N = 525$K. Our computations were carried out in the paramagnetic phase, which is not problematic, since the gap opened by electronic correlations does not depend on whether the system is magnetically ordered. It has been shown in angle-resolved photoemission experiments (ARPES), that passing the Néel temperature does not qualitatively alter the valence band spectrum [51].

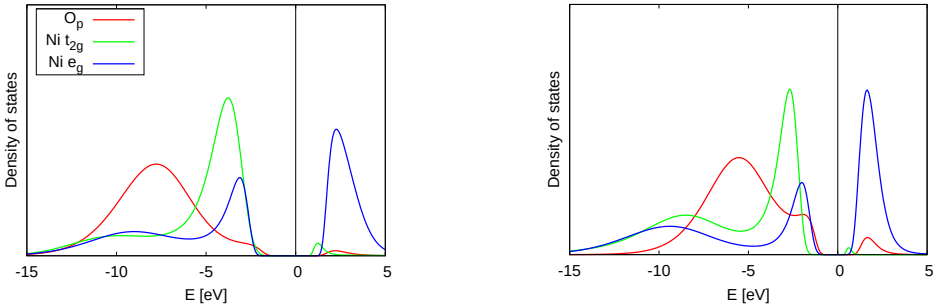

(a) $\mu_{dc} = 21\text{eV}$, $\mu = 3.0\text{eV}$ (b) $\mu_{dc} = 25\text{eV}$, $\mu = 0.5\text{eV}$

Figure 5.3: Spectral functions at $\beta = 5\text{eV}^{-1}$ for different values of the double counting μ_{dc} obtained with LDA+DMFT (QMC).

5.3 Methodology and Results

The model that has to be used for a simulation of NiO is the five band Hubbard model which describes the correlated $3d$ states of Ni. We have calculated the model parameters of such a model in an *ab initio* fashion. The local orbitals are represented by Wannier functions, which have been shown recently [52, 53, 54] to be a very good choice for a basis set, because they form a complete basis of the Hilbert space spanned by Bloch functions and are reminiscent of localized atomic orbitals. Our calculations involved two different flavours of the LDA+DMFT framework: One uses a projection of Bloch states on local orbitals represented by Wannier functions [55, 54] and a Quantum Monte Carlo (QMC) solver [21], while the other employs the Linear Order Muffin-Tin Orbital method (LMTO) [7] and a finite-temperature exact diagonalization (ED) solver [56, 57].

The effective Wannier Hamiltonian includes the five $3d$ bands of nickel as the correlated subspace and the three $2p$ bands of oxygen as the uncorrelated part. The inclusion of the p bands is physically motivated since in a charge transfer compound the oxygen bands play an important role in the physics of the system, as was pointed out above. A computation taking into account only the Ni d states is capable of reproducing the insulating behavior and the size of the gap as shown by Ren et al. [41]. Additionally, the double counting is reduced to a trivial shift in calculations that contain only the Ni d bands, since the full Wannier Hamiltonian belongs to the correlated subspace. The double counting can thus be absorbed into the total chemical potential. However, the physics of the charge transfer insulator cannot be captured without taking into account the ligand p states.

Our calculations were performed at inverse temperature $\beta = 5\text{eV}^{-1}$,

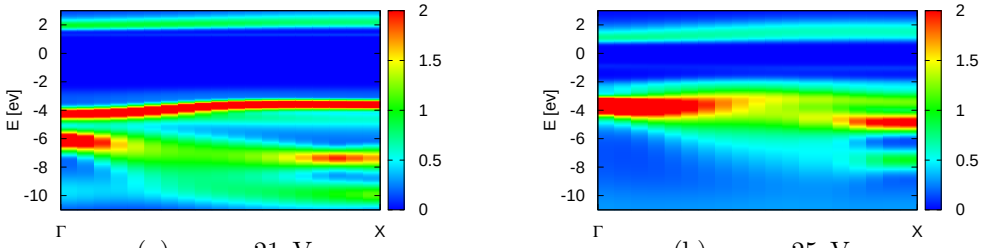

(a) $\mu_{dc} = 21$eV (b) $\mu_{dc} = 25$eV

Figure 5.4: **k**-resolved spectral functions $A(\mathbf{k}, \omega)$ along the line Γ—X in the Brillouin zone for different values of the double counting μ_{dc} obtained using LDA+DMFT (QMC).

which corresponds to 2321K, using up to 80 time slices and on the order of $\sim 10^6$ Monte Carlo sweeps in the QMC. In the ED fraction of calculations we used a ten site cluster (5 impurity levels and 5 bath levels). The temperature used may appear high, yet it is low enough to give a qualitatively correct description of the physics of the material. Computations at lower temperatures pose no fundamental problem, the amount of LDA+DMFT calculations performed for this study would have made them too expensive though. We have used a Coulomb interaction matrix corresponding to the parameter values $U = 8$eV and $J = 1$eV.

The double-counting potential μ_{dc} defined above is found to have profound impact on the density of states $N_i(\omega) = -\frac{1}{\pi} G_i(\omega)$ shown in Fig.(5.3) and the **k**-resolved spectral function
$A_i(\mathbf{k}, \omega) = -\frac{1}{\pi} \mathrm{Im} \left(\omega + \mu - \varepsilon_i(\mathbf{k}) - \Sigma_i(\omega)\right)^{-1}$ shown along the line Γ—X in the Brillouin zone in Fig.(5.4). The spectral functions were obtained by the maximum entropy method [58] from imaginary time Green functions. The double-counting potential has been treated here as an adjustable parameter and has been varied between 21eV and 26eV. These values already contain the intrinsic shift due to the energy of the particle-hole symmetry in the Hirsch-Fye QMC method that amounts to 34eV with our values of U and J. The energy of the particle-hole symmetry is obtained from Eq.(5.1) with $n^0 = \frac{1}{2}$.

The most prominent effects of the double counting on the spectral properties are the shift of the oxygen p bands with respect to the nickel d bands, as well as the variation in gap size. Plainly speaking, the double-counting correction allows for a tuning of the spectral properties from a large gap Mott-Hubbard insulator to a metal. The regime of the charge transfer insulator, the expected physical state of NiO, lies somewhere in between. The experimental spectrum, obtained by x-ray-photoemission (PES) and

bremsstrahlung-isochromat-spectroscopy (BIS) showing both occupied and unoccupied parts, was obtained by e.g. Sawatzky and Allen [50]. The spectrum recorded at 120eV is predominantly of Ni $3d$ character, while the 66eV spectrum contains a strong contribution of O $2p$ at about -4eV [50, 59]. Additionally, the detailed decomposition of the spectra showed contributions of both O $2p$ and Ni $3d$ at the top of the valence band [50, 59]. The calculated LDA+DMFT(QMC) spectral function shown in Fig.(5.3) show basically the two different physical situations of a Mott-Hubbard Fig.(5.3(a)) and a charge-transfer insulator Fig.(5.3(b)) mentioned above. Both spectral functions were obtained for NiO, by varying the double-counting correction. The characteristic feature of a charge-transfer system, the strongly hybridized ligand p and transition metal d character of the low-energy charge excitations [45, 50], is only present in the spectrum in Fig.(5.3(b)). The spectrum in Fig.(5.3(a)) is missing this feature almost completely and shows Mott-Hubbard behavior. This difference underscores the importance of the proper choice for the double-counting correction.

Let us now turn to the $\mathbf{k}$-resolved spectral functions shown in Fig.(5.4) and compare them with ARPES data [60, 61]. The uppermost band in Figs.(5.4(a), 5.4(b)) at $\sim$ 2eV above the Fermi level is a Ni e_g band, while the other bands can be identified with the ones obtained by ARPES. The two lowest lying bands correspond to oxygen p states, the bands above are formed by Ni d states. The characteristic features seen in ARPES, like the broadening of the oxygen bands around the midpoint of the Γ—X line, are clearly present. The quantitative features, especially the relative band energies can strongly differ, depending on the double counting chosen. The bands in Fig.(5.4(a)) ($\mu_{dc} = 21$eV) show a clear separation between the oxygen and the nickel part at the Γ-point as well as the X-point. At the increased value of the double counting $\mu_{dc} = 25$eV the oxygen bands are shifted towards the Fermi level, coming to overlap with the Ni d bands at the Γ point as in the ARPES data. A detailed comparison of the calculated bandstructures with experiments shows that the bands calculated with $\mu_{dc} = 25$eV agree very well with the experimental data. These calculations reproduce the flat bands at -4eV and another at about -2eV becomes more prominently visible at $\mu_{dc} = 25$eV, while it is very faint at $\mu_{dc} = 21$eV. The dispersive bands in the region -4eV to -8eV also agree very well with experiment. Our calculations at this value of μ_{dc} yield very similar results as those obtained by Kuneš et al. [43]. Calculations with other values of the double counting can strongly differ from the experimental data, as shown by the example of $\mu_{dc} = 21$eV in Fig.(5.4(a)).

The dimension of the problem of the double counting becomes apparent

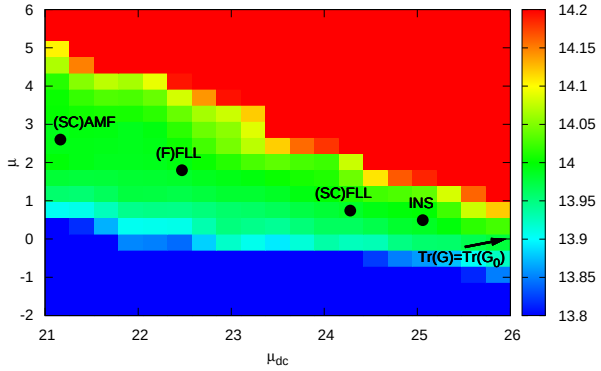

Figure 5.5: Surface created by different combinations of the chemical potential μ and the double-counting potential μ_{dc} plotted versus the particle number N obtained with LDA+DMFT (QMC). The particle number has been color coded: the green plateau corresponds to a particle number very close to the desired value of $N = 14$, values below are encoded in blue, values above in red. Additionally the results produced by different methods to fix the double counting are indicated. For the AMF and FLL functionals SC or F in parentheses indicates, that the self-consistent occupancies from the DMFT or the formal occupancies have been used respectively. For further details we refer to the text.

if the parameter space of the overall chemical potential μ and the double-counting potential μ_{dc} versus the total particle number in the system N is examined. The result is shown in Fig.(5.5) with the particle number color coded. The picture shows that in principle any combination of μ and μ_{dc} that yields a point in the green plateau, corresponding to the desired particle number $N = 14$ a priori describes the system equivalently good. The problem that arises here is that conventionally fixing the total chemical potential μ in the middle of the gap still leaves one the freedom of choosing different values for μ_{dc}. An additional condition is required to completely determine the systems position in the (μ, μ_{dc}) parameter space and thus in the end its spectral properties. As we have argued above this choice is of crucial relevance for the results of the LDA+DMFT simulation and not just an unimportant technicality. Since other, related approaches, like the LDA+U method, also include a double counting the problem is not new. Over the years different analytic methods to fix μ_{dc} have been devised. Two prominent examples are the around mean-field (AMF) [62] approximation and the fully localized or atomic limit (FLL) [63]. The AMF is based on the conjecture that LDA corresponds to a mean-field solution of the many-body problem, as was argued by Anisimov et al. [62]. The resulting double-counting potential

is

$$\mu_{dc}^{AMF} = \sum_{m'} U_{mm'} n^0 + \sum_{m',m' \neq m} (U_{mm'} - J_{mm'}) n^0, \tag{5.1}$$

where $n^0 = \frac{1}{2(2l+1)} \sum_{m,\sigma} n_{m\sigma}$ is the average occupancy. We use the global average and not the spin dependent version proposed in Ref.[63], since we were performing paramagnetic calculations in which both spin components are equally occupied. One assumes all orbitals belonging to a certain value of the angular momentum l to be equally occupied and subtracts a corresponding mean-field energy. This is, however, incorrect, since LDA contains the crystal field splitting explicitly and will in general not produce equally occupied orbitals even for weakly correlated systems. The result for the case of NiO using self-consistent occupancies from the DMFT loop is shown in Fig.(5.5) labeled (SC)AMF. The value obtained with the formal occupancies given above ((F)AMF) lies outside of the considered part of the parameter space at 20.4eV. In both cases the solution corresponds in our case to a Mott-Hubbard insulator as shown in Fig.(5.3(a)). The AMF functional is known to produce unsatisfactory results for strongly correlated systems, which led to the development of another method, the so called FLL.

The FLL functional takes the converse approach to the AMF and begins with the atomic limit. It has been shown, that this new potential can be written as a correction of the AMF solution (5.1) in the following form [63]

$$\mu_{dc}^{FLL} = \mu_{dc}^{AMF} + (U - J)(n^0 - \tfrac{1}{2}).$$

This addition to the AMF potential has the effect of a shift of the centroid of the level depending on its occupation. An empty level is raised in energy by $\frac{1}{2}(U - J)$ and the converse happens to a fully occupied level. The form of the functional is based on the property of the *exact* density functional that the one electron potential should jump discontinuously at integer electron number [64], which is not fulfilled in LDA or GGA. Ultimately the FLL leads to a stronger trend towards integer occupancies and localization. The result of the FLL, as shown in Fig.(5.5), constitutes a substantial improvement over AMF, yet still produces too low values. The general problem with analytic expressions like the ones presented is that their scope is limited to certain classes of systems that fulfill the assumptions made in the derivation process. The AMF for example might give good results for weakly correlated systems, but it certainly fails for the strongly correlated ones. The FLL improves the situation for insulators, but it is still based on ad-hoc assumptions. Additionally a certain degree of ambiguity is inherent, since one can compute the corrections using the formal occupancies given above, occupancies obtained from LDA or from the self-consistent DMFT loop. Other analytical formulas

for the double-counting correction have been proposed for the case of NiO, see e.g. the work by Korotin et al. [44] and Kuneš et al. [42]. Despite giving reasonable resulting spectral functions analytical approaches to the double counting are not optimal.

The obvious problems with analytical formulas make conceptually different approaches worth exploring. It would certainly be an improvement if the double counting could be found self-consistently along with the chemical potential in the DMFT self-consistency loop. Since the double counting correction is intrinsically an impurity quantity and not a global quantity (like the chemical potential μ) it would be most desirable to use intrinsic quantities of the impurity like the impurity self-energy or the impurity Green function to fix it. One possible ansatz using the impurity self-energy $\Sigma^{imp}_{mm'}$ is to constraint the high energy tails in the real part of the self-energy to sum up to zero

$$\mathrm{ReTr}(\Sigma^{imp}_{mm'}(i\omega_N)) \stackrel{!}{=} 0.$$

Here, ω_N is the highest Matsubara frequency included in the computation. Physically this amounts to the requirement that the shift in the centroid of the impurity orbitals contains no static component. The resulting correction is $\mu_{dc} \sim 21.3$eV and thus very close to the (SC)AMF value shown in Fig.(5.5). The result produced is thus reasonable in principle in the sense that it produces an insulating solution. However, the resulting spectrum resembles a Mott-Hubbard system. Double counting corrections based on the self-energy have been applied successfully to metallic systems, see e.g. [65].

Another very promising approach, which is in principle based on the Friedel sum rule [66], is to constraint the total charge in the impurity. This approach requires that the electronic charge computed from the local noninteracting Green function and the one computed from the interacting impurity Green function are identical [55]

$$\mathrm{Tr}\ G^{imp}_{mm'}(\beta) \stackrel{!}{=} \mathrm{Tr}\ G^{0,loc}_{mm'}(\beta). \tag{5.2}$$

Alternatively one can also use the Weiss field $\mathcal{G}_{mm'}$ instead of the local noninteracting Green function in above equation. Both versions of the method give very similar results and work very well in metallic systems [55], since in a metal the total particle number of the system N and of the impurity n_{imp} are both very sensitive to small variations in μ and μ_{dc}. As NiO has a quite large gap the charge does almost not vary with neither the chemical nor the double-counting potential in the gap. The constraint of fixed particle number can thus be fulfilled to a very good approximation in the whole gap region, the criterion (5.2) essentially breaks down. Since the gap in NiO is large

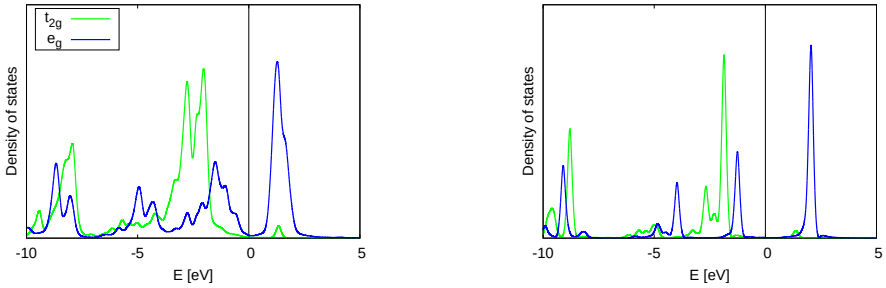

(a) Lattice (b) Cluster

Figure 5.6: Ni $3d$ spectral functions at $\beta = 5\text{eV}^{-1}$ for $\mu_{dc} = 25.3\text{eV}$ obtained by LDA+DMFT (ED).

this method fails and drives the system towards a metallic state at double counting $\mu_{dc} \sim 26.5\text{eV}$ indicated by the arrow pointing out of Fig.(5.5).

Since the double-counting corrections that we have explored either fail to reproduce the physics of NiO or are based on analytic arguments that do not exactly apply to the system a different, sound way fixing the value of the double counting for insulating systems is needed. Since the double-counting potential effectively acts like an impurity chemical potential we propose to find the value at which it lies in the middle of the gap of the impurity spectral function where the occupation of the impurity is about $n_{imp} \approx 8$ particles. This part of the calculations was done using the exact diagonalization impurity solver (see above), which is much faster and uses the full Coulomb interaction matrix including spin-flip and pair-hopping terms. Additionally it does not suffer from statistical errors and directly provides data on the real axis. We used a 10 site cluster with 5 impurity levels plus 5 bath levels and fit the bath Green function via the level energies and hopping parameters [57]. An explicit scan of the parameter space revealed that the proper value for the double-counting correction is $\mu_{dc} \sim 25\text{eV}$, basically the same value found above by inspection and comparison of spectral features to experimental data. It is indicated as INS in Fig.(5.5). The corresponding lattice and cluster spectral functions are shown in Fig.(5.6). The proposed criterion thus produces a double-counting correction that reproduces the spectral features of the valence in accord with photoemmission measurements and does not contain ad-hoc assumptions about the system.

Chapter 6

Satellite in Ni

6.1 Introduction

Electron correlations in transition metals are a basic problem in itinerant electron ferromagnetism [67]. One way of tackling this problem is by doing band calculations within the local-density approximation (LDA) [40]. The LDA is known to work rather well for ground state properties of transition metals. However, it does not have a firm theoretical ground with respect to excited states. One well-known shortcomings of the LDA in describing excited states is known to exist for ferromagnetic nickel, where it overestimates the band width and the exchange splitting [68, 69] , and where the calculated energy dispersion does not agree with the quasiparticle bands determined by angular resolved photoemission experiments [70, 71, 72, 73] . In addition, the LDA is unable to reproduce satellite peaks in the photoemission spectra, like the one found around 6 eV below the Fermi level. There has been an attempt to improve the situation by using the GW expansion [74] . Although the quasiparticle energies are much improved, the exchange splitting is not improved and the problem of reproducing the satellite peaks at 6 eV still remains.

Another way is the mapping of the lattice problem onto an effective impurity problem which is solved numerically exactly. The local self-energy is then determined via a self-consistency procedure. This is called dynamical mean-field theory (DMFT) [8].

The many-body impurity problem can be solve, in the case of single-band systems, by using techniques such as numerical renormalization group [75, 76] (NRG), exact diagonalization [56] (ED), quantum Monte Carlo [21] (QMC), or other schemes [23] . For computational reasons dynamical correlations in realistic multiband materials have so far been investigated mainly within

QMC [77] ,iterative perturbation theory [78, 39] (IPT), and the fluctuation exchange method (FLEX) [79, 80]. The versatility of the QMC approach is made feasible by allowing only Ising-like exchange interaction to avoid serious sign problems at low temperatures [81] . Extensions of QMC including full Hund's exchange are presently limited to $T = 0$ and rather high temperatures ($T > 1500$). Spin-flip interactions at low finite temperatures can be taken into account in two recently developed schemes [82, 83], namely the continuous-time QMC method [84, 85] and the combination of the Hirsch-Fye algorithm with a perturbation series expansion .

The aim of this chapter is to demonstrate that multiband ED/DMFT is a highly useful scheme for the investigation of Coulomb correlations [86, 87] in realistic materials.

6.2 Methodology and Results

Let us consider nickel as material whose single-particle properties are characterized by a Hamiltonian $H(k)$, obtained within LMTO (see 4.2). We take into account $4p$,$4s$, and $3d$ orbitals so the Hamiltonian is a 9×9 matrix. The purpose of single-site DMFT [88] is to derive a local self-energy $\Sigma(\omega)$ which describes the modification of the single-particle bands caused by Coulomb interactions. The local Green's function in orthogonal basis is given by the expression

$$G_{\alpha\beta}(i\omega_n) = \sum_k [\hat{1}(i\omega_n + \mu) - \hat{H}(k) - \Sigma(i\omega_n)]^{-1}_{\alpha\beta}, \tag{6.1}$$

where $\omega_n = (2n+1)/\pi k_B T$ are the Matsubara frequencies, μ is the chemical potential adjusted to the total number of particle $N_{total} = 10$ ($4p^0 4s^2 3d^8 [Ar]$ - electron configuration for nickel)

$$N = \int_{-\infty}^{\mu} N(\varepsilon) d\varepsilon, \tag{6.2}$$

α, β denotes correspond orbitals, $\hat{1}$ - unity matrix, $\Sigma(i\omega_n)$ - block-diagonal matrix where only the part corresponded to d-orbitals contains nonzero elements.

The LMTO Hamiltonian is obtained by means of numerical orthogonalization of Eq. (2.38)

Nickel is a cubic crystal and we can choose cubic basis to simplify the notations. In this basis Green's function is diagonal, i.e. (6.1) could be rewritten as

$$G_m(i\omega_n) = \sum_k [\hat{1}(i\omega_n + \mu) - \hat{H}(k) - \Sigma(i\omega_n)]^{-1}_m \tag{6.3}$$

Since the Green's function has poles near the real axis we perform the DMFT iterations on Matsubara frequencies. After convergence is reached we make extra one iteration on real energy to obtain a spectral density function $\rho(E)$.

Within the DMFT quantum impurity calculations it is necessary to remove the self-energy from the central site. Using Dyson equation for this purpose we obtain the bath Green's function

$$G_m^0(i\omega_n) = [G_m(i\omega_n)^{-1} + \Sigma_m(i\omega_n)]^{-1} \tag{6.4}$$

Within ED/DMFT the lattice bare Green's function is approximated via an Anderson impurity model for a cluster Green's function, where the cluster consists of impurity levels $\varepsilon^{imp}_{m=1,\ldots,5}$ and bath levels $\varepsilon^{bath}_{k=1,\ldots,5}$ coupled via hopping matrix elements V_{mk}. That model is represented on Fig. 6.1.

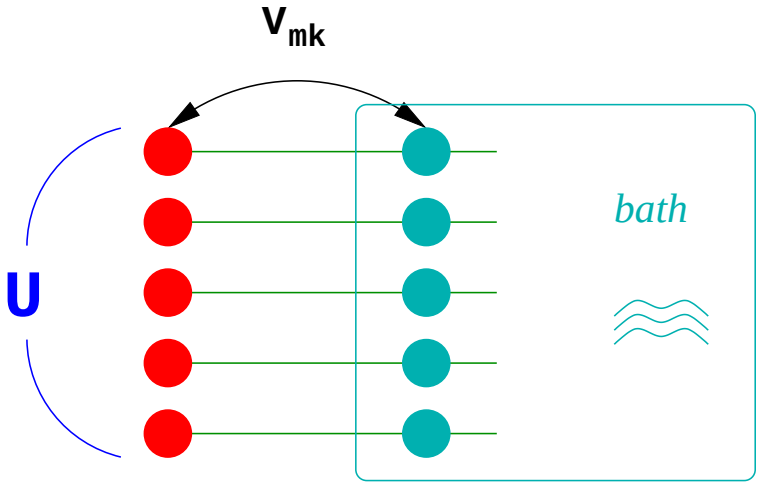

Figure 6.1: Impurity Anderson Model with $N_s = 10 \quad N_{imp} = 5 \quad N_{bath} = 5$

Thus

$$G_m^0(i\omega_n) \approx G_m^{0,imp}(i\omega_n), \tag{6.5}$$

where

$$G_m^{0,imp}(i\omega_n) = \left(i\omega_n - \varepsilon_m^{imp} - \sum_{k=1}^{N_{bath}} \frac{|V_{mk}|^2}{i\omega_n - \varepsilon_k^{bath}} \right)^{-1}. \tag{6.6}$$

Here N_{bath} is a number of bath orbitals. We use a diagonal bath in our

calculations, i.e.

$$V_{mk} = \begin{cases} V_{t_{2g}}, & k = m = t_{2g} \\ V_{e_g}, & k = m = e_g \\ 0, & k \neq m. \end{cases} \tag{6.7}$$

Let us rewrite (6.6) as:

$$G_m^{0,imp}(i\omega_n)^{-1} = i\omega_n - \varepsilon_m^{imp} - \Delta_m(i\omega_n), \tag{6.8}$$

where $\Delta_m(i\omega_n)$ is a hybridization function:

$$\Delta_m(i\omega_n) = \sum_k^{N_{bath}} \frac{|V_{mk}|^2}{i\omega_n - \varepsilon_k} \tag{6.9}$$

For convenience denote

$$\tilde{\Delta}_m(i\omega_n) = \varepsilon_m^{imp} + \Delta_m(i\omega_n) \tag{6.10}$$

Then ε_m^{imp} are evaluated to obey the relation

$$Re\,\tilde{\Delta}_m(\omega \to \infty) = 0 \tag{6.11}$$

Only ε_k^{bath}, V_{mk} parameters are used in fitting procedure to fulfill the relation (6.5). Actually the DMFT remains a freedom to coincide $G_m^0(i\omega_n)$ and $G_m^{0,imp}(i\omega_n)$. We chose the following relation

$$\sum_{i\omega_n,m} \left| \left[G_m^0(i\omega_n)\right]^{-1} - \left[G_m^{0,imp}(i\omega_n)\right]^{-1} \right| \Longrightarrow min \tag{6.12}$$

After all impurity parameters are obtained we construct Hamiltonian for 5-band Anderson impurity model

$$H_{AIM} = \sum_{m\sigma}(\varepsilon_m - \mu_{dc}) n_{m\sigma} + \sum_{mk\sigma}[V_{mk} c_{m\sigma}^+ c_{k\sigma} + h.c.] + \frac{1}{2}\sum_{\sigma,\sigma'}\sum_{ijkl} U_{ijkl} c_{i\sigma}^+ c_{j\sigma'}^+ c_{l\sigma'} c_{k\sigma}, \tag{6.13}$$

where $c_{m\sigma}^{(+)}$ are annihilation (creation) operators for electrons in impurity level $m \leq 5$ with spin σ and $n_{m\sigma} = c_{m\sigma}^+ c_{m\sigma}$ with similar notation. h.c. denotes

Hermitian conjugate terms. U_{ijkl} is a matrix element of local atomic-like Coulomb interaction [89, 90]

$$U_{ijkl} = \int d\boldsymbol{r} d\boldsymbol{r}' \phi_i^*(\boldsymbol{r}) \phi_j^*(\boldsymbol{r}') u_c(\mathbf{r} - \mathbf{r}') \phi_k(\boldsymbol{r}) \phi_l(\boldsymbol{r}'), \tag{6.14}$$

where $u_c(\mathbf{r} - \mathbf{r}')$ is the screened Coulomb interaction and the functions $\phi_i(\boldsymbol{r})$ from a basis of correlated subspace. In order to calculate $U_{mm'}$ and $J_{mm'}$ one should know the Slater integrals F^k (F^0,F^2,F^4 for d electrons) [90, 89, 62]. The Coulomb parameter U (6.15) could be identified with the Slater integral F^0. Using properties of the Clebsch-Gordan coefficients one can obtain

$$\bar{U} = \frac{1}{(2l+1)^2} \sum_{ij} U_{ijij} = F^0 \tag{6.15}$$

$$\begin{aligned} \bar{U} - \bar{J} &= \frac{1}{(2l+1)2l} \sum_{ij} U_{ijij} - U_{ijji} \\ &= F^0 - (F^2 + F^4), \end{aligned} \tag{6.16}$$

$$\bar{J} = \frac{F^2 + F^4}{14} \tag{6.17}$$

For convinced we accept $\bar{U} \equiv U$ and $\bar{J} \equiv J$. To define all three Slater integrals from U and J one needs to know only the ratio F^2/F^4. This ratio for all ions($3d$ elements) is between 0.62 and 0.63. So fixed the ratio at 0.625. Then the expressions for the Slater integrals are

$$\begin{aligned} F^2 &= \frac{14}{1.625} J \\ F^4 &= 0.625 F^2 \end{aligned} \tag{6.18}$$

Parameter μ_{dc} is double counting parameter. It is fixed due to relation $N_{Ni}^{ED} \approx 8$ and depends only from Coulomb interaction. Here N_{Ni}^{ED} is calculated after H_{AIM} is diagonalized and eigenvectors and eigenvalues are found

$$N_{Ni}^{ED} = \sum_{m\sigma} \sum_{\nu} \langle \nu | c_{m\sigma}^+ c_{m\sigma} | \nu \rangle \tag{6.19}$$

μ_{dc} is defined approximately in one iteration before self-consistent calculation starts.

The Hamiltonian (6.13) is to be diagonalize by temperature Lanczos method. The details of this method was specified in detailed in chapter

4. Here we just note that parameter $N_{ranoldi}$(the number of eigenstates taken into account) was allowed to 20. It is sufficient at the temperature of calculations $\beta = 10$.

The impurity Green's function is evaluated based on found eigenvalues and eigenstates and using temperature Lanczos only with $c^+|\nu\rangle$, $c|\nu\rangle$ ($\hat{H}_{AIM}|\nu\rangle = E_\nu|\nu\rangle$)as initial vectors (see 4.2):

$$G^{imp}(iw_n) = \frac{1}{Z}\sum_\nu e^{-\beta E_\nu}[G^>(iw_n) + G^<(iw_n)],$$

where

$$G^{\nu>}(iw_n) = \cfrac{\langle\nu|c\,c^+|\nu\rangle}{iw_n - a_0^> - \cfrac{{b_1^>}^2}{iw_n - a_1^> - \cfrac{{b_2^>}^2}{iw_n - a_2^> \cdots}}}$$

$$G^{\nu<}(iw_n) = \cfrac{\langle\nu|c^+c|\nu\rangle}{iw_n + a_0^< - \cfrac{{b_1^<}^2}{iw_n + a_1^< - \cfrac{{b_2^<}^2}{iw_n + a_2^< \cdots}}}$$

and coefficients $a_i^>$, $a_i^<$, $b_i^>$, $b_i^<$ are obtained due to (4.15) (see chapter 4.2). In analogy to (6.4) the cluster self-energy is calculated due to the expression:

$$\Sigma_m^{imp}(i\omega_n) = G_m^{0,imp}(i\omega_n)^{-1} - G_m^{imp}(i\omega_n)^{-1} \tag{6.20}$$

And in the spirit of DMFT [91] we make approximation that the impurity self-energy coincides with the lattice self-energy

$$\Sigma_m(i\omega_n) \approx \Sigma_m^{imp}(i\omega_n) \tag{6.21}$$

The exact diagonalization method involves a projection of the bath Green's function $\mathcal{G}_0$ onto the space of functions $\{\mathcal{G}_0^{N_s}\}$ built out of N_s orbitals. This projection operation is not smooth and can lead to convergence brake. To avoid it we mix actual self-energy with previous one

$$\Sigma_m^{act}(i\omega_n) = \alpha\Sigma_m^{act}(i\omega_n) + (1-\alpha)\Sigma_m^{prev}(i\omega_n) \tag{6.22}$$

The coefficient α could vary. We assign it to $\alpha = 0.5$.

Now the loop could be schematically represented as

$$\Sigma \to G \to G_0 \approx G_0^{imp} \to G^{imp} \to \Sigma^{imp} \approx \Sigma. \tag{6.23}$$

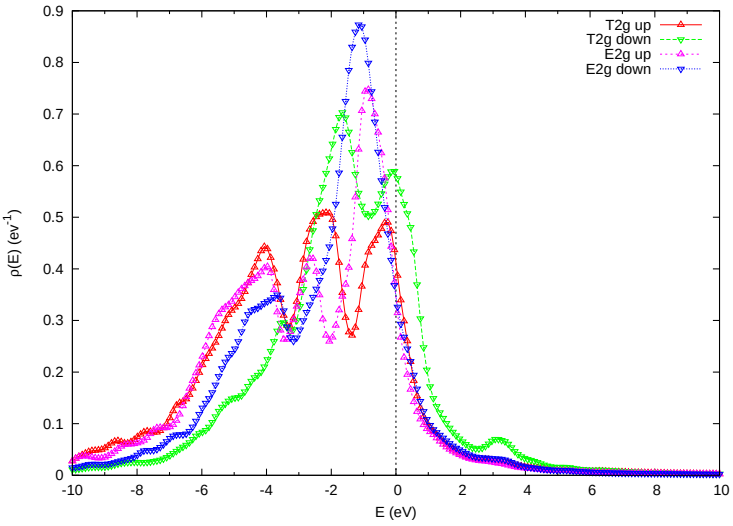

Figure 6.3: Density of states for nickel. Temperature Lanczos method were used for Anderson impurity model 5+5. $\beta = 10\,eV^{-1}$ $U = 3.5\,eV$ $J = 0.9\,eV$

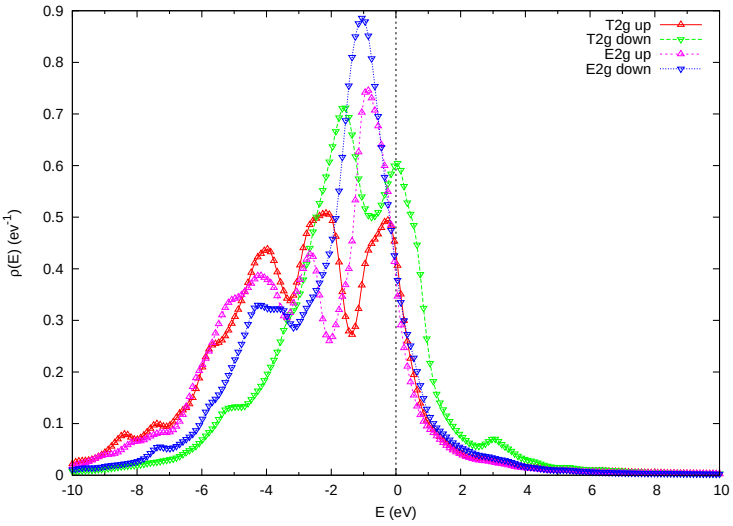

Figure 6.4: Density of states for nickel. Temperature Lanczos method were used for Anderson impurity model 5+5. $\beta = 10\,eV^{-1}$ $U = 3.0\,eV$ $J = 0.9\,eV$

The calculations was made for three values of U $3.0\,eV$, $3.5\,eV$, $4.0\,eV$ and correspondingly μ_{dc} $21.00\,eV$, $25.40\,eV$, $29.60\,eV$. Exchange Coulomb parameter $J = 0.9\,eV$, and inverse temperature $\beta = 10\,eV$. Because of the problem with fitting procedure (on the stage $G^{0,lattice} \approx G^{0,cluster}$) we made self-consistent calculation for paramagnetic system and only after convergence is reached we perform one iteration for magnetic system with fixed hybridization parameters only introducing spin polarization manually $|\Delta\varepsilon_{k\sigma}| = |\varepsilon_{k\uparrow} - \varepsilon_{k\downarrow}| = 0.4\,eV$

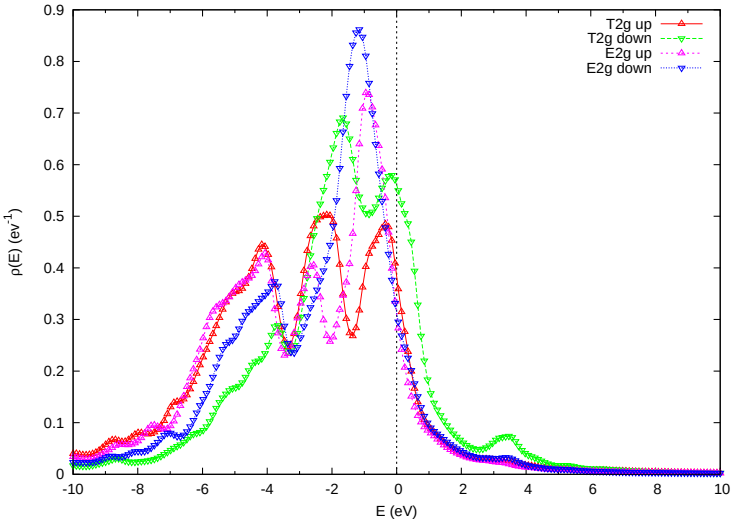

Figure 6.2: Density of states for nickel. Temperature Lanczos method were used for Anderson impurity model 5+5. $\beta = 10\,eV^{-1}$ $U = 4.0\,eV$ $J = 0.9\,eV$

On Fig. 6.4 one can see satellite around $-5\,eV$. It is not well resolved and not spin-polarized. We suppose that the resolution of the satellite pick could be improved by increasing the bath discretization. The problem of spin-polarization is expected to be solve with the program version supplied spin-polarized fitting procedure.

Chapter 7

Conclusions and Outlook

Different numerical approaches in a solid state physics allow to investigate systems which could be hardly treated by analytical methods due to complexity [92] or nonperturbative character of the problem [93, 16].

Dynamical mean-field theory (DMFT) [23] has provided an efficient tool to treat systems with strong electronic calculations. There are two most useful methods used as an impurity solver (to solve eigenproblem for Anderson impurity model) within the DMFT: Quantum Monte Carlo (QMC) and Exact diagonalization (ED). While each of them has its advantages [94, 95] the only ED-family methods supply the calculation of Green's function on real energy scale, while the QMC evaluates the Green's function on imaginary time and therefore entails with a problem of analytical continuation. Moreover the ED-scheme allows to see directly the complicated multiplet structure of the system. The freedom concerns the geometry of the electronic bath, and the physical parameters of the orbitals (the site energies and hopping amplitudes) is another benefit of this method.

In the present thesis the temperature Lanczos method is presented. This technique provides calculations of spectral functions at finite temperatures. The method was implemented to model systems presented by clusters described Anderson impurity models such as $5+1$ and $5+5$. It was shown that even for zero temperature a set of eigenstates has to be taken into account for proper account for orbital degeneracy. So the temperature Lanczos method could be called degenerate Lanczos method.

The finite temperature Lanczos technique was also implemented to real compounds such nickel and nickel oxide. For the nickel $5+5$ AIM is used. At the time when these calculations were made the fitting procedure for finding parameters of Anderson impurity model could not work with spin-polarized system. So self-consistent calculations were made in nonmagnetic regime. After convergence were reached one spin-polarized iteration with fixed bath

parameters were carried out. The bath is diagonal, so each impurity orbital connects with it its own bath. It brings our model closer to reality but from other side only one bath orbital for each impurity site is taken into account. The single-particle Green's function for ferromagnetic nickel has been calculated and satellite pick in the spectral function were found about $-5\,eV$. We suppose that exactly the small bath discretization leads to not very well resolved satellite pick in spectral function. We found that the satellite pick is hardly spin-polarized. It is required to improve the fitting procedure to deal with spin-polarized bath and we hope that will improve the results.

For nickel oxide we showed that the double-counting correction in the LDA+DMFT formalism has to be very carefully assessed when performing calculations with a correlated and uncorrelated part in the Hamiltonian. We have examined the influence of the double-counting potential on the spectral properties using the example of NiO. Different tracks in the search for a sound double counting were explored. A well defined analytical expression for the double-counting potential μ_{dc} probably cannot be formulated in the context of LDA+DMFT. Thus, one has to resort to numerical criteria to fix the value of the double-counting correction. For metals the self consistency criterion based on the charge Eq.(5.2) works very reliably. It is, however, not applicable to insulating systems. In such a case we proposed to fix the value of the double-counting potential by setting it in the middle of the gap of the impurity spectral function. This criterion led to spectral properties in good agreement with experiments. Thus, one has to resort to self-consistent numerical approaches to fix the double-counting correction properly. Further work, especially the examination of other systems will show if the proposed methodology can be reliably applied to predict the electronic structure of correlated electron systems by LDA+DMFT calculations.

Bibliography

[1] L.H.Thomas. *The calculations of atomic fields.* Proc. Cambridge Phil. Roy. Soc., 1927.

[2] E.Fermi. *Un metodo statisticoper la determinazione di alcuna priorieta dell'atome.* Rend.Accad.Naz.Lincei, 1927.

[3] P.A.M.Dirac. *Note on exchange phenomena in the Thomas-Fermi atom.* Proc. Cambridge Phil. Roy. Soc., 1930.

[4] P. Hohenberg and W. Kohn. Inhomogeneous electron gas. *Phys. Rev.*, 136(3B):B864–B871, Nov 1964.

[5] J.W.Strutt(Lord Rayleigh). *Theory of sounds.* Reprint: Dover Publications, 1945.

[6] W.Ritz. *Über eine neue Methode zur Lossung GewisserVariationsprobleme der Mathematischen Physik.* Reine Angew. Math., 1908.

[7] O. Krogh Andersen. *Phys. Rev. B*, 12(8):3060–3083, Oct 1975.

[8] G. Kotliar, S. Y. Savrasov, K. Haule, V. S. Oudovenko, O. Parcollet, and C. A. Marianetti. Electronic structure calculations with dynamical mean-field theory. *Rev. Mod. Phys.*, 78(3):865, 2006.

[9] Antoine Georges and Gabriel Kotliar. Hubbard model in infinite dimensions. *Phys. Rev. B*, 45(12):6479–6483, Mar 1992.

[10] Elliott H. Lieb and F. Y. Wu. The one-dimensional hubbard model: a reminiscence. *Physica A: Statistical Mechanics and its Applications*, 321(1-2):1 – 27, 2003. Statphys-Taiwan-2002: Lattice Models and Complex Systems.

[11] J. Hubbard. Electron Correlations in Narrow Energy Bands. *Proceedings of the Royal Society of London. Series A. Mathematical and Physical Sciences*, 276(1365):238–257, 1963.

[12] J. Hubbard. Electron Correlations in Narrow Energy Bands. II. The Degenerate Band Case. *Proceedings of the Royal Society of London. Series A. Mathematical and Physical Sciences*, 277(1369):237–259, 1964.

[13] J. Hubbard. Electron Correlations in Narrow Energy Bands. III. An Improved Solution. *Proceedings of the Royal Society of London. Series A. Mathematical and Physical Sciences*, 281(1386):401–419, 1964.

[14] E. Müller-Hartmann. Self-consistent perturbation theory of the anderson model: ground state properties. *Z. Phys. B*, 57(4):281, 1984.

[15] S K Sarker. A new functional integral formalism for strongly correlated fermi systems. *Journal of Physics C: Solid State Physics*, 21(18):L667–L672, 1988.

[16] Walter Metzner and Dieter Vollhardt. Correlated lattice fermions in $d = \infty$ dimensions. *Phys. Rev. Lett.*, 62(3):324–327, Jan 1989.

[17] J.E. Gubernatis H.Q. Lin. Exact diagonalization methods for quantum systems. *Computers in Physics*, 7(4):400–407, 1993.

[18] H. Fehske E. Jeckelmann. Exact numerical methods for electron-phonon problems. *arXiv:0510637 v2*, 2005.

[19] Salvatore R. Manmana Reinhard M. Noack. Diagonalization- and numerical renormalization-group-based methods for interacting quantum systems. *arXiv:0510321 v1*, 2005.

[20] Christopher Z. Mooney. *Monte Carlo simulation (Quantitative Applications in the Social Sciences)*. Sage, Thousand Oaks, California, 1997.

[21] J. E. Hirsch and R. M. Fye. Monte carlo method for magnetic impurities in metals. *Phys. Rev. Lett.*, 56(23):2521–2524, Jun 1986.

[22] D. J. Scalapino and R. L. Sugar. Method for performing monte carlo calculations for systems with fermions. *Phys. Rev. Lett.*, 46(8):519–521, Feb 1981.

[23] Antoine Georges, Gabriel Kotliar, Werner Krauth, and Marcelo J. Rozenberg. Dynamical mean-field theory of strongly correlated fermion systems and the limit of infinite dimensions. *Rev. Mod. Phys.*, 68(1):13, Jan 1996.

[24] A. N. Rubtsov. Quantum monte carlo determinantal algorithm without hubbard-stratonovich transformation: a general consideration. *arXiv:0302228, unpublished*, 2003.

[25] A. N. Rubtsov and A. I. Lichtenstein. Continuous-time quantum monte carlo method for fermions: Beyond auxiliary field framework. *JETP Lett.*, 80:61 – 65, 2004.

[26] J. E. Hirsch. Discrete hubbard-stratonovich transformation for fermion lattice models. *Phys. Rev. B*, 28(7):4059–4061, Oct 1983.

[27] J. Sherman and W. J. Morrison. Adjustment of an inverse matrix corresponding to a change in one element of a given matrix. *The Annals of Mathematical Statistics*, 21(1):124–127, March 1950.

[28] A. A. Abrikosov, L. P. Gor'kov, and I. E. Dzyaloshinskii. *Methods of Quantum Field Theory in Statistical Physics*. Pergamon Press, New York, 1965.

[29] Gerald D. Mahan. *Many-particle Physics*. Kluwer Academic Publishers, New York, 2000.

[30] A. B. Migdal. *Theory of finite Fermi Systems and applications to atomic nuclei*. Interscience Publishers, New York, 1967.

[31] D.G. Pettifor D.L. Weaire. *The Recursion method ans Its Applications*. Springer, 1985.

[32] C. Lanczos. *J.Res.Nat.Bur.Stand.*, 1950.

[33] Intel math kernel library. http://software.intel.com/en-us/intel-mkl/.

[34] *Linear Algebra Package(lapack, fortran and c libraries; an implementation of the blas library is required for this package), http://www.netlib.org/lapack*.

[35] *Basic Linear Algebra Subprograms(blas, frotran libraries providing basic matrix and vector operations), http://www.netlib.org/blas*.

[36] Elbio Dagotto and Adriana Moreo. Improved hamiltonian variational technique for lattice models. *Phys. Rev. D*, 31(4):865–870, Feb 1985.

[37] Eduardo R. Gagliano, Elbio Dagotto, Adriana Moreo, and Francisco C. Alcaraz. Erratum: Correlation functions of the antiferromagnetic heisenberg model using a modified lanczos method. *Phys. Rev. B*, 35(10):5297–5298, Apr 1987.

[38] Arpack – arnoldi package. http://www.caam.rice.edu/software/ARPACK/.

[39] V I Anisimov, A I Poteryaev, M A Korotin, A O Anokhin, and G Kotliar. *Journal of Physics: Condensed Matter*, 9(35):7359–7367, 1997.

[40] A. I. Lichtenstein and M. I. Katsnelson. Ab initio calculations of quasiparticle band structure in correlated systems: Lda++ approach. *Phys. Rev. B*, 57(12):6884–6895, Mar 1998.

[41] X. Ren, I. Leonov, G. Keller, M. Kollar, I. Nekrasov, and D. Vollhardt. *Phys. Rev. B*, 74(19):195114, 2006.

[42] J. Kuneš, V. I. Anisimov, A. V. Lukoyanov, and D. Vollhardt. *Phys. Rev. B*, 75(16):165115, 2007.

[43] J. Kuneš, V. I. Anisimov, S. L. Skornyakov, A. V. Lukoyanov, and D. Vollhardt. *Phys. Rev. Lett.*, 99(15):156404, 2007.

[44] Dm. Korotin, A. V. Kozhevnikov, S. L. Skornyakov, I. Leonov, N. Binggeli, V. I. Anisimov, and G. Trimarchi. *The European Physical Journal B*, 65(1):91–98, sep 2008.

[45] Masatoshi Imada, Atsushi Fujimori, and Yoshinori Tokura. *Rev. Mod. Phys.*, 70(4):1039–1263, Oct 1998.

[46] J. Zaanen, G. A. Sawatzky, and J. W. Allen. *Phys. Rev. Lett.*, 55(4):418–421, Jul 1985.

[47] A. E. Bocquet, T. Mizokawa, K. Morikawa, A. Fujimori, S. R. Barman, K. Maiti, D. D. Sarma, Y. Tokura, and M. Onoda. *Phys. Rev. B*, 53(3):1161–1170, Jan 1996.

[48] P. E. Blöchl. *Phys. Rev. B*, 50(24):17953–17979, Dec 1994.

[49] G. Kresse and D. Joubert. *Phys. Rev. B*, 59(3):1758–1775, Jan 1999.

[50] G. A. Sawatzky and J. W. Allen. *Phys. Rev. Lett.*, 53(24):2339–2342, Dec 1984.

[51] O. Tjernberg, S. Söderholm, G. Chiaia, R. Girard, U. O. Karlsson, H. Nylén, and I. Lindau. *Phys. Rev. B*, 54(15):10245–10248, Oct 1996.

[52] V. I. Anisimov, D. E. Kondakov, A. V. Kozhevnikov, I. A. Nekrasov, Z. V. Pchelkina, J. W. Allen, S.-K. Mo, H.-D. Kim, P. Metcalf, S. Suga, A. Sekiyama, G. Keller, I. Leonov, X. Ren, and D. Vollhardt. *Phys. Rev. B*, 71(12):125119, 2005.

[53] E. Pavarini, S. Biermann, A. Poteryaev, A. I. Lichtenstein, A. Georges, and O. K. Andersen. *Phys. Rev. Lett.*, 92(17):176403, Apr 2004.

[54] F. Lechermann, A. Georges, A. Poteryaev, S. Biermann, M. Posternak, A. Yamasaki, and O. K. Andersen. *Phys. Rev. B*, 74(12):125120, 2006.

[55] B. Amadon, F. Lechermann, A. Georges, F. Jollet, T. O. Wehling, and A. I. Lichtenstein. *Phys. Rev. B*, 77(20):205112, 2008.

[56] Michel Caffarel and Werner Krauth. *Phys. Rev. Lett.*, 72(10):1545–1548, Mar 1994.

[57] Massimo Capone, Luca de' Medici, and Antoine Georges. *Phys. Rev. B*, 76(24):245116, Dec 2007.

[58] Mark Jarrell and J. E. Gubernatis. *Physics Reports*, 269(3):133 – 195, 1996.

[59] D. E. Eastman and J. L. Freeouf. *Phys. Rev. Lett.*, 34(7):395–398, Feb 1975.

[60] Z.-X. Shen, C. K. Shih, O. Jepsen, W. E. Spicer, I. Lindau, and J. W. Allen. *Phys. Rev. Lett.*, 64(20):2442–2445, May 1990.

[61] Z.-X. Shen, R. S. List, D. S. Dessau, B. O. Wells, O. Jepsen, A. J. Arko, R. Barttlet, C. K. Shih, F. Parmigiani, J. C. Huang, and P. A. P. Lindberg. *Phys. Rev. B*, 44(8):3604–3626, Aug 1991.

[62] Vladimir I. Anisimov, Jan Zaanen, and Ole K. Andersen. Band theory and mott insulators: Hubbard u instead of stoner i. *Phys. Rev. B*, 44(3):943–954, Jul 1991.

[63] M. T. Czyżyk and G. A. Sawatzky. *Phys. Rev. B*, 49(20):14211–14228, May 1994.

[64] V. I. Anisimov, I. V. Solovyev, M. A. Korotin, M. T. Czyżyk, and G. A. Sawatzky. *Phys. Rev. B*, 48(23):16929–16934, Dec 1993.

[65] J. Braun, J. Minár, H. Ebert, M. I. Katsnelson, and A. I. Lichtenstein. *Physical Review Letters*, 97(22):227601, 2006.

[66] A. C. Hewson. *The Kondo problem to heavy fermions*. Cambridge University Press, 1997.

[67] A. I. Lichtenstein, M. I. Katsnelson, and G. Kotliar. Finite-temperature magnetism of transition metals: An ab initio dynamical mean-field theory. *Phys. Rev. Lett.*, 87(6):067205, Jul 2001.

[68] J. Callaway and C. S. Wang. Energy bands in ferromagnetic iron. *Phys. Rev. B*, 16(5):2095–2105, Sep 1977.

[69] J.F.Janak. A.R.Williams V. L. Moruzzi. *Calculated Electronic Properties of Metals*. Pergamon, 1978.

[70] D. E. Eastman, F. J. Himpsel, and J. A. Knapp. Experimental band structure and temperature-dependent magnetic exchange splitting of nickel using angle-resolved photoemission. *Phys. Rev. Lett.*, 40(23):1514–1517, Jun 1978.

[71] F. J. Himpsel, J. A. Knapp, and D. E. Eastman. Experimental energy-band dispersions and exchange splitting for ni. *Phys. Rev. B*, 19(6):2919–2927, Mar 1979.

[72] D. E. Eastman, F. J. Himpsel, and J. A. Knapp. Experimental exchange-split energy-band dispersions for fe, co, and ni. *Phys. Rev. Lett.*, 44(2):95–98, Jan 1980.

[73] H. Mårtensson and P. O. Nilsson. Investigation of the electronic structure of ni by angle-resolved uv photoelectron spectroscopy. *Phys. Rev. B*, 30(6):3047–3054, Sep 1984.

[74] F. Aryasetiawan. Self-energy of ferromagnetic nickel in the gw approximation. *Phys. Rev. B*, 46(20):13051–13064, Nov 1992.

[75] Kenneth G. Wilson. The renormalization group: Critical phenomena and the kondo problem. *Rev. Mod. Phys.*, 47(4):773–840, Oct 1975.

[76] Ralf Bulla, Theo A. Costi, and Thomas Pruschke. Numerical renormalization group method for quantum impurity systems. *Rev. Mod. Phys.*, 80(2):395, 2008.

[77] S. Savrasov G. Kotliar. *New Theoretical Approches to Strongly Correlated Systems*. Kluwer Academic Publishers, 2001.

[78] L. Craco, M. S. Laad, and E. Müller-Hartmann. Orbital kondo effect in $cro2$: A combined local-spin-density-approximation dynamical-mean-field-theory study. *Phys. Rev. Lett.*, 90(23):237203, Jun 2003.

[79] N. E. Bickers, D. J. Scalapino, and S. R. White. Conserving approximations for strongly correlated electron systems: Bethe-salpeter equation and dynamics for the two-dimensional hubbard model. *Phys. Rev. Lett.*, 62(8):961–964, Feb 1989.

[80] N. E. Bickers and D. J. Scalapino. Conserving approximations for strongly fluctuating electron systems. i. formalism and calculational approach. *Annals of Physics*, 193(1):206 – 251, 1989.

[81] E. Y. Loh, J. E. Gubernatis, R. T. Scalettar, S. R. White, D. J. Scalapino, and R. L. Sugar. Sign problem in the numerical simulation of many-electron systems. *Phys. Rev. B*, 41(13):9301–9307, May 1990.

[82] A. N. Rubtsov. Small parameter for lattice models with strong interaction. *arXiv:0601333, unpublished*, 2006.

[83] A. Fuhrmann, S. Okamoto, H. Monien, and A. J. Millis. Fictive-impurity approach to dynamical mean-field theory: A strong-coupling investigation. *Phys. Rev. B*, 75(20):205118, 2007.

[84] Tudor D. Stanescu and Gabriel Kotliar. Strong coupling theory for interacting lattice models. *Phys. Rev. B*, 70(20):205112, Nov 2004.

[85] A. N. Rubtsov, V. V. Savkin, and A. I. Lichtenstein. Continuous-time quantum monte carlo method for fermions. *Phys. Rev. B*, 72(3):035122, Jul 2005.

[86] Tudor D. Stanescu and Philip Phillips. Nonperturbative approach to full mott behavior. *Phys. Rev. B*, 69(24):245104, Jun 2004.

[87] Tudor D. Stanescu, Philip Phillips, and Ting-Pong Choy. Theory of the luttinger surface in doped mott insulators. *Phys. Rev. B*, 75(10):104503, 2007.

[88] Gabriel Kotliar and Dieter Vollhardt. Strongly correlated materials: Insights from dynamical mean-field theory. *Physics Today*, 57(3):53–59, 2004.

[89] Takashi Miyake and F. Aryasetiawan. Screened coulomb interaction in the maximally localized wannier basis. *Phys. Rev. B*, 77(8):085122, Feb 2008.

[90] Vladimir I Anisimov, F Aryasetiawan, and A I Lichtenstein. First-principles calculations of the electronic structure and spectra of strongly

correlated systems: the lda + u method. *Journal of Physics: Condensed Matter*, 9(4):767, 1997.

[91] Gordon Baym. Self-consistent approximations in many-body systems. *Phys. Rev.*, 127(4):1391–1401, Aug 1962.

[92] F. J. Ohkawa. Mott metal-insulator transition in the hubbard model. *arXiv:0707.0142, unpublished*, 2007.

[93] N. F. Mott. *Metal-Insulator Transitions*. Taylor and Francis, London, 1974.

[94] Matthias Troyer and Uwe-Jens Wiese. Computational complexity and fundamental limitations to fermionic quantum monte carlo simulations. *Phys. Rev. Lett.*, 94(17):170201, May 2005.

[95] Jaebeom Yoo, Shailesh Chandrasekharan, Ribhu K Kaul, Denis Ullmo, and Harold U Baranger. On the sign problem in the hirsch & fye algorithm for impurity problems. *Journal of Physics A: Mathematical and General*, 38(48):10307–10310, 2005.

Acknowledgements

I would like to express my gratitude to all the people who gave me assistance and support during my work at the *1 Institut für Theoretische Physik*.

First of all, I would like to thank my supervisor, Prof. Alexander Lichtenstein, for giving me the opportunity to study such interesting areas of modern computational physics. I am thankful for the interesting topic proposed, for many helpful discussions during the work, and for patienly explaining the basics of many-body physics.

I would like to thanks also my previous supervisor, Prof. Sergey Ovchinnikov for discussion complicated quastions of theoretical physics, whatever complicated they were and for good recomendations which allowed me to take the PhD position in Prof. Lichtenstein's group.

I am grateful to Prof. Erik Koch for very fruitful discussions while visiting Jülich Forschungzentrum. As a result of this discussion the part devoted to analizing the multiplet structure of model systems was improved.

I would like to express my special appreciation to Prof. Frank Lechermann for help in all starting from computational problems to complicated quastions of many-body physics.

I am very grateful to Dr. Vladimir Mazurenko for help in work of adaptation the ARPACK libraries package to the code realizing finite temperature Lanczos technique. And I am greatly indebt to Alexander Poteryaev for help in embedding the finite temperature Lanczos code in the program realized LDA+DMFT calculations.

I give special thanks to Dr. Evgeny Gorelov, Dr. Hartmut Hafermann, Dr.Tim Wehling, Dr. Ivan Leonov and Dr. Sergey Brener for help programming and in practice work at this thesis.

I want also acknoledge Sergej Schuwalow for very interesting discussions of defferent quastions of theoretic physics and for his inestimable help in German language.

I acknowledge Michael Karolak for productive colloboration during work at double-counting problem in nickel oxide.

I would like to thank all the membes of my committee: Dr. Alexander

Chudnovskiy, Prof. Erik Koch, Prof. Frank Lechermann, Prof. Michael Potthoff and Dr. Hartmut Haffermann for the time and energy they have devoted to reading my thesis and for disputation during my defence.